JMS-DX303 spectrometer and a JEOL JMS-T100LC. ^1H and ^{13}C NMR spectra were measured with JEOL JNM-A500 and JEOL JNM-ECA600 spectrometers, using DMSO-d_6 as the solvent and TMS as an internal reference.

X-ray Crystallography. X-ray crystallographic measurements were performed on a Rigaku AFC7R diffractometer, with graphite monochromated Cu Kα radiation and a rotating anode generator. Calculations of the measurements were performed using the teXan crystallographic software package (Molecular Structure Corporation).

Preparation of 10-Hydroxyl-11-oxo-1,N2-ethano-dGuo. dGuo (27 mg, 0.1 mmol) and glyoxylic acid monohydrate (9 mg, 0.1 mmol) were dissolved in 1 mL of DMSO and incubated at 45 °C for 4 days. The reaction mixture was diluted 10-fold with water, and the major product was purified by repeated rounds of HPLC (CAPCELL PAK C18, 10 mm × 250 mm; elution, 4% acetonitrile in water), to yield 8.8 mg (27%) of the objective compound.

Synthesis of (*E*)-4-Oxo-2-hexenal(4-OHE). (*E*)-4-Hydroxy-2-hexenal diethylacetal (19.7 g, 104 mmol), prepared by the method of Esterbauer and Weger (*12*), was dissolved in dry dichloromethane (500 mL), and then, activated MnO_2 (240 g, Aldrich) was added to the solution. After a 72 h incubation at room temperature, the reaction mixture was filtered, washed with dichloromethane (500 mL), and concentrated under reduced pressure. The residue was fractionated by silica gel column chromatograpy [column volume, 450 mL; elution, first with hexane and then with hexane:ethyl acetate (9:1, v/v)] to yield 13.9 g (71%) of the pale yellow product of 4-OHE diethylacetal. It was dissolved in a mixture of 70 mL of 1% citric acid and 30 mL of methanol and was stirred for 24 h at room temperature. The methanol was evaporated under reduced pressure, and then, the solution was saturated with NaCl and extracted with ether. The ether layer was washed with a saturated NaCl solution and dried with anhydrous $MgSO_4$. The ether layer was concentrated under reduced pressure to obtain 5.7 g (68%) of 4-OHE. Mass (EI), *m/z* 112. NMR ($\delta CDCl_3$, *J*) 9.79 ppm (d, 6.9 Hz), 6.90 ppm (d, 16.2 Hz), 6.79 ppm (dd, 6.9, 16.2 Hz), 2.74 ppm (q, 7.2 Hz), 1.17 ppm (t, 7.2 Hz).

Preparation of 10-(2-Oxobutyl)-1,N2-etheno-dGuo. dGuo (40.9 mg, 0.15 mmol) and 4-OHE (25.8 mg, 0.23 mmol) were dissolved in 8.2 mL of 50 mM sodium phosphate buffer (pH 7.4) containing 10% ethanol and incubated for 5 days at room temperature. The major product was purified by repeated rounds of HPLC (CAPCELL PAK C18, 10 mm × 250 mm; elution, 10% acetonitrile in water) to yield 28.8 mg (63%) of the objective compound.

Preparation of 9-Ethyl-10-(2-oxobutyl)-1,N2-ethenoguanine. 9-Ethylguanine (30 mg, 0.17 mmol) and 4-OHE (28.2 mg, 0.25 mmol) were dissolved in 8.2 mL of 50 mM sodium phosphate buffer (pH 7.4) containing 10% ethanol and incubated for 5 days at room temperature. The major product was purified by repeated rounds of HPLC (the same conditions as above) to yield 31.5 mg (57%) of the objective compound. Mass spectrum (FAB), $(M - H)^-$, *m/z* 272.1145 (272.1148, calcd for $C_{13}H_{14}N_5O_2$).

X-ray Crystallographic Analysis of 9-Ethyl-10-(2-oxobutyl)-1,N2-ethenoguanine (7). A colorless plate crystal, with approximate dimensions of 0.02 mm × 0.13 mm × 0.40 mm, was chosen for X-ray crystallography. The crystal data are as follows: empirical formula, $C_{13}H_{15}N_5O_2$; crystal system, monoclinic; lattice parameters, a = 13.996(1) Å, b = 7.401(1) Å, c = 14.643(1) Å, β = 114.756(6)°, V = 1377.4(3) Å^3; Z value, 4; D_{calcd}, 1.32 g/cm^3. μ (Cu Kα): 7.71 cm^{-1}. Of the 4914 reflections that were collected, 2352 were unique. The intensities of three representative reflections were measured after every 150 reflections. No decay correction was applied. The structure was solved by direct methods (SIR92) (*13*) and was expanded using Fourier techniques (DIRDIF94) (*14*). Nonhydrogen atoms were refined anisotropically. Hydrogen atoms were included but not refined. The final cycle of full matrix least-squares refinement was based on 2047 observed reflections and 181 variable parameters and was converged with unweighted and weighted agreement factors of R = 0.082 and Rw = 0.159. The maximum and minimum peaks on the final difference Fourier map corresponded to 0.34 and −0.17e$^-$/Å^3, respectively.

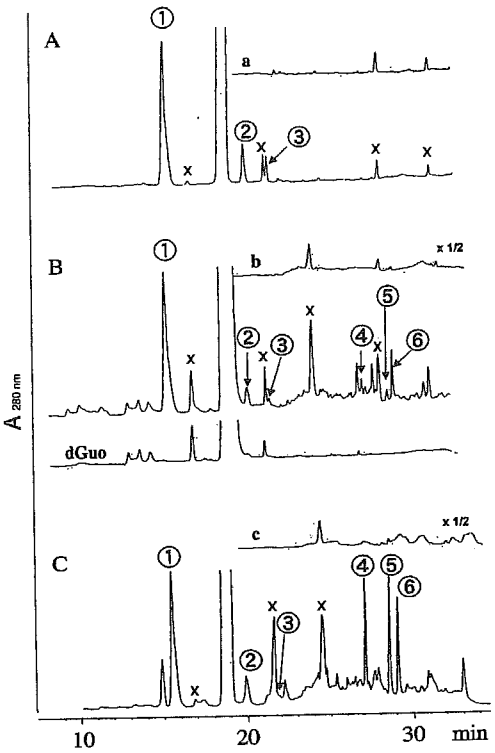

Figure 1. HPLC analyses of dGuo adducts formed by model lipid peroxidation reactions. (A) dGuo + MLA + hemin, (a) control reaction of MLA + hemin; (B) dGuo + salad oil + hemin, (b) control reaction of salad oil + hemin (attenuation, 1/2), (dGuo) control reaction of dGuo; (C) dGuo + MLN + hemin, (c) control reaction of MLN + hemin (attenuation, 1/2). The peaks labeled with x were also detected in the control reaction mixtures.

Mutagenicity Test. The bacterial mutagenicity test was carried out according to the method of Maron and Ames (*15*). In our experiments, we used a longer preincubation time, 60 min, and the plates were sealed with paraffin film (Parafilm, American National Can, United States) to prevent the evaporation of 4-OHE.

Results

Identification of Mutagens as dGuo Adducts Formed in Lipid Peroxidation Model Reactions. The method generally used to identify lipid peroxide-derived mutagens is to isolate them by HPLC, based on their mutagenic activity, before their structure determination. However, in the initial studies, we were not able to isolate unstable lipid peroxide-derived mutagens by HPLC. An alternative method to identify unstable mutagens is to trap them as stable dGuo adducts, because many mutagens and carcinogens react with DNA and nucleosides, particularly dGuo (*16*).

Using this method, the products formed in the model lipid peroxidation reaction mixtures (MLA + hemin, MLN + hemin, and salad oil + hemin), which are models of high-fat and red meat diets, were reacted with dGuo by vigorous shaking to form a homogeneous emulsion at a physiological pH (7.4). The reaction mixture was fractionated by HPLC coupled to a photodiode array UV detector. Six dGuo adducts, which were not produced from the control reaction mixtures of dGuo only or lipid peroxidation only (−dGuo), were detected by HPLC, as shown in Figure 1.

Adducts 1 and 2 were produced in both the MLA and the MLN reactions (Figure 1), while adducts 4−6 were detected in the MLN reaction mixture (Figure 1C). The amounts and the numbers of different adducts were higher in the MLN reaction mixture (Figure 1C) than the MLA reaction mixture (Figure

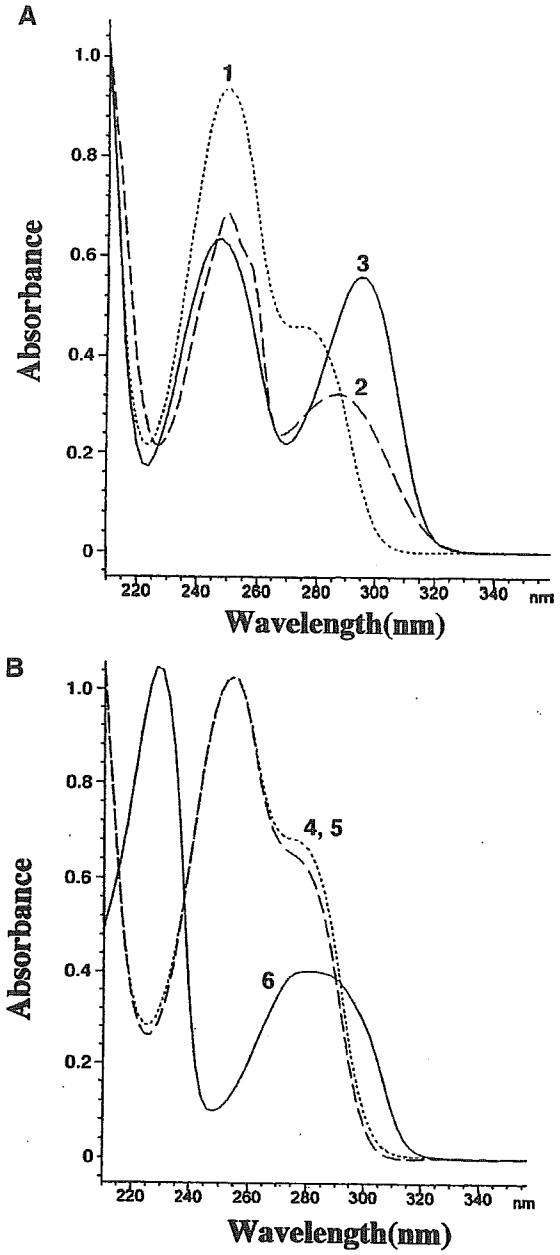

Figure 2. UV spectra of dGuo adducts. (A) Adducts 1 (• • •), 2 (- - -), and 3 (—); (B) adducts 4 (- - -), 5 (• • •), and 6 (—).

1A). Adduct 3 (8-OH-dGuo) was produced with a higher yield in the MLA reaction (Figure 1A) than in the MLN reaction (Figure 1C). The salad oil reaction generated an HPLC profile (Figure 1B) including some adducts also generated in the MLA (Figure 1A) and MLN reactions (Figure 1C).

Structure Determinations of Adducts. Adduct 1 was easily identified as glyoxal-dGuo (Figure 3, structure **1**), based on its characteristic UV spectrum (λ_{max}, 249 nm, shoulder at 275 nm) (Figure 2A-1). This identification was confirmed by a comparison with the synthetic compound prepared from glyoxal and dGuo (*18*–*20*).

The mass spectrum, $(M - H)^-$, *m/z* 322.0787 (322.0788, calcd for $C_{12}H_{12}N_5O_6$) of adduct 2 showed an increase of 56 mass units (C_2O_2) from dGuo. One of the possible structures was a cyclic adduct formed from glyoxylic acid and dGuo. Thus, compound **2** was prepared as a major reaction product of glyoxylic acid and dGuo. The retention time in HPLC and the ^{1}H NMR, UV, and mass spectral data of adduct 2 were identical to those of the synthetic **2**. The ^{13}C and ^{1}H NMR data of

Table 1. ^{13}C and ^{1}H NMR Assignments for Compound 2[a]

	δC (ppm)	δH (ppm)	multiplicity	J (Hz)
1N				
2	151.47			
3N				
4	147.88, 147.91			
5	120.32, 120.38			
6	154.24			
7N				
8	136.67, 136.70	8.14	s	
9N				
10	77.61	5.71	d	9.0
		5.72	d	9.0
11	171.25			
12N				
1′	83.12	6.17	dd	6.4, 6.0
2′	39.84	2.27	dddd	13.4, 6.0, 3.0, 3.0
		2.55	br. dd	13.4, 6.4
3′	70.55	4.35	m	
4′	87.84	3.83	m	
5′	61.51	3.52	m	
10 OH		7.81	d	9.0
		7.83	d	9.0
3′OH		5.31	br d	
5′OH		4.92	br t	

[a] 1′–5′, numbering of sugar carbons.

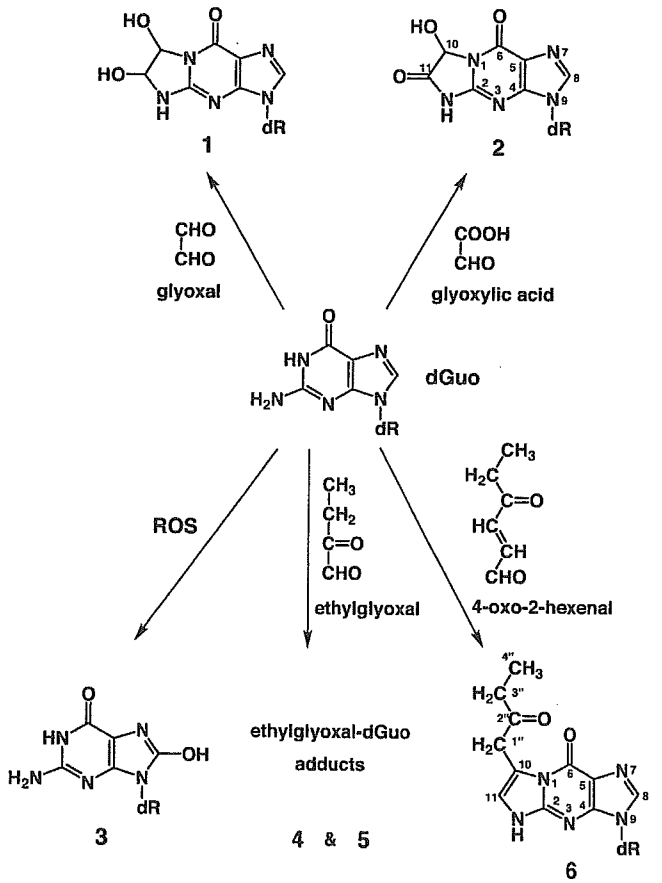

Figure 3. Structures of dGuo adducts formed by model lipid peroxidation reactions and their causative mutagens.

synthetic **2** are shown in Table 1. The proposed structure **2** was confirmed by ^{1}H–^{1}H two-dimensional (2D) correlation spectroscopy (COSY) and ^{1}H–^{13}C 2D heteronuclear multiple-bond correlation (HMBC) NMR studies using synthetic **2** (Figures 4 and 5). The three-bond correlation between H-10, C-10, N-1, and C-6 observed in the HMBC spectrum (Figure 5) clearly shows that adduct 2 is an 11-oxo-10-hydroxy compound, and the possibility of the regioisomer, the 11-hydroxy-10-oxo compound, should be ruled out.

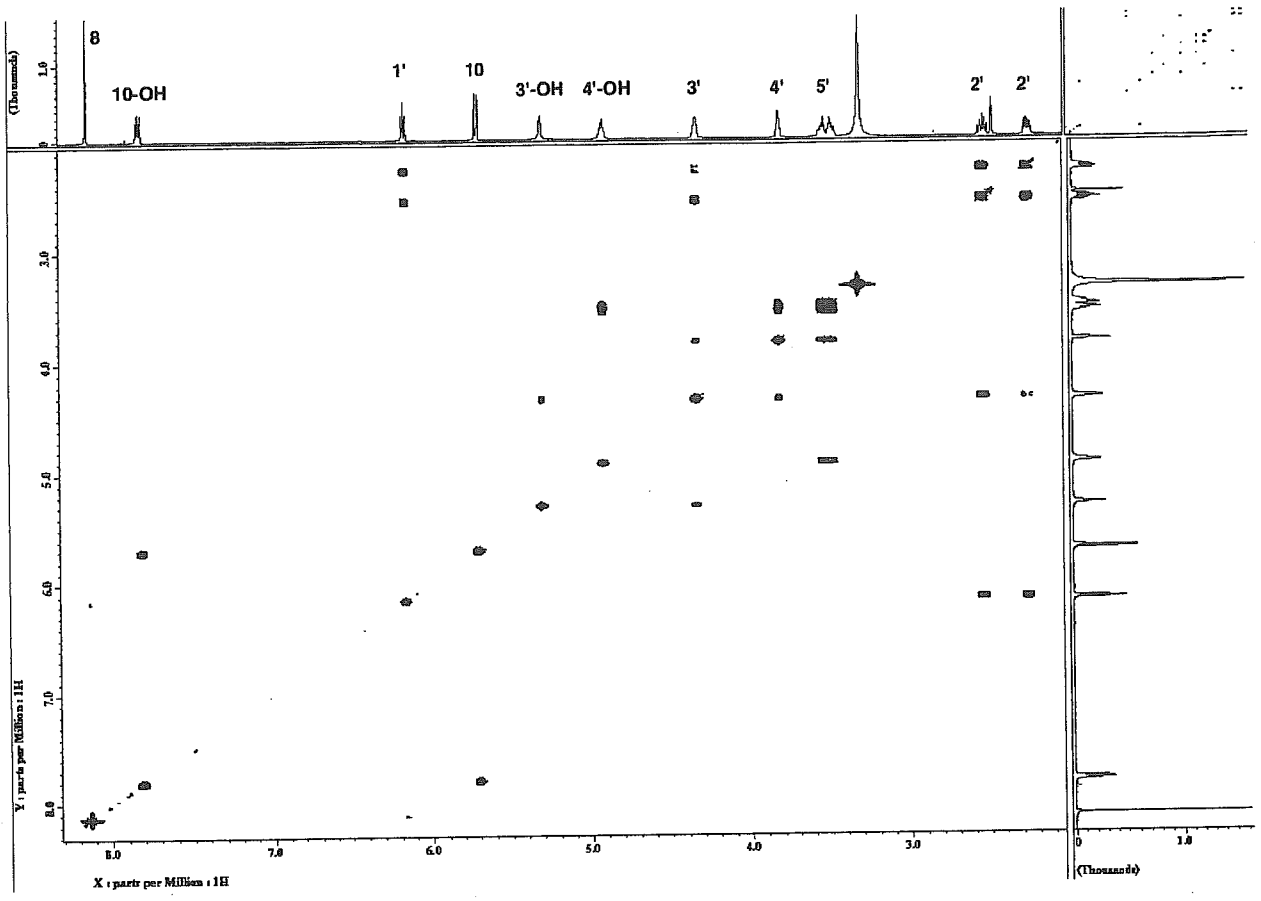

Figure 4. $^{1}H-^{1}H$ 2D COSY NMR spectrum of compound **2**.

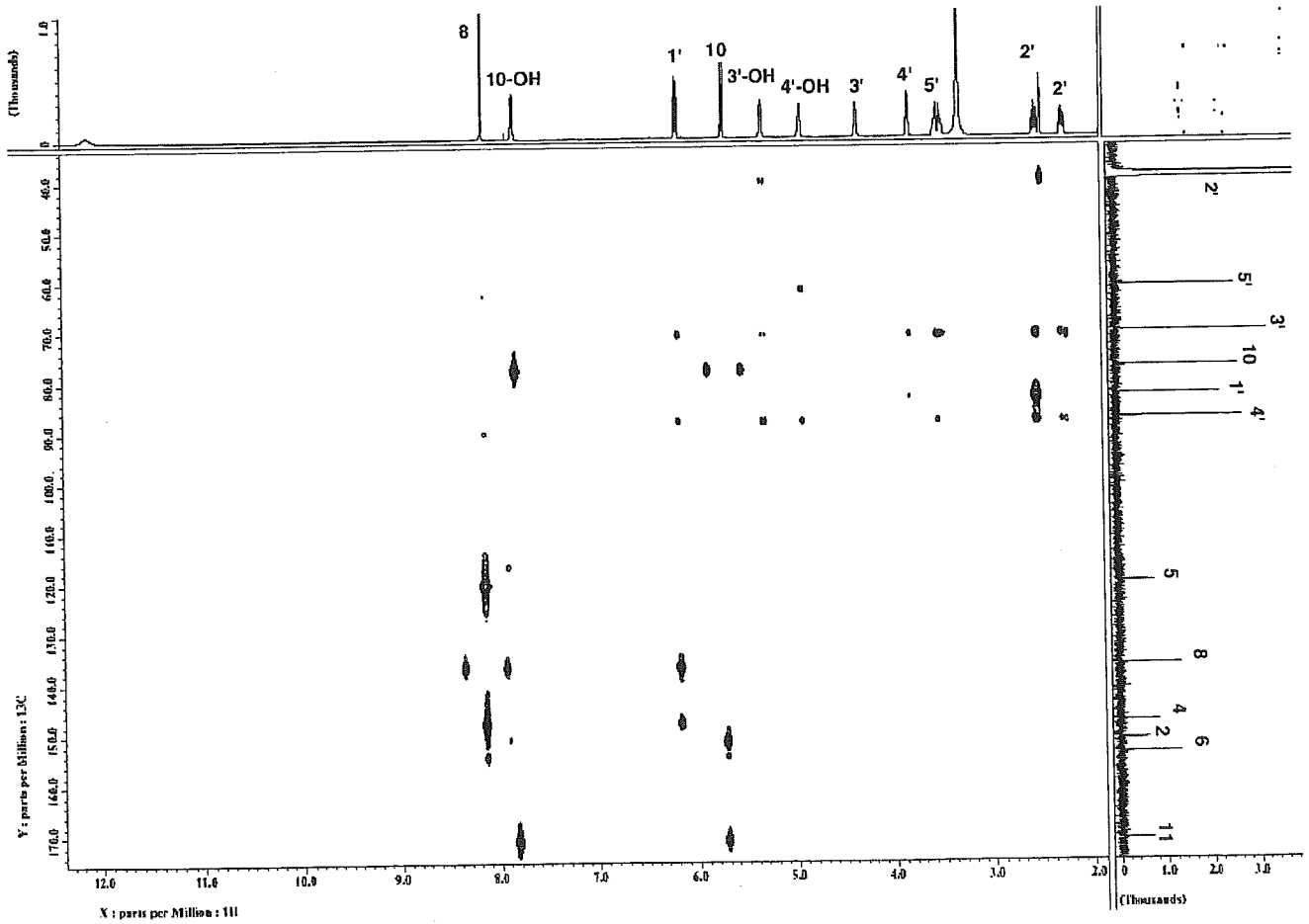

Figure 5. $^{1}H-^{13}C$ 2D HMBC NMR spectrum of compound **2**.

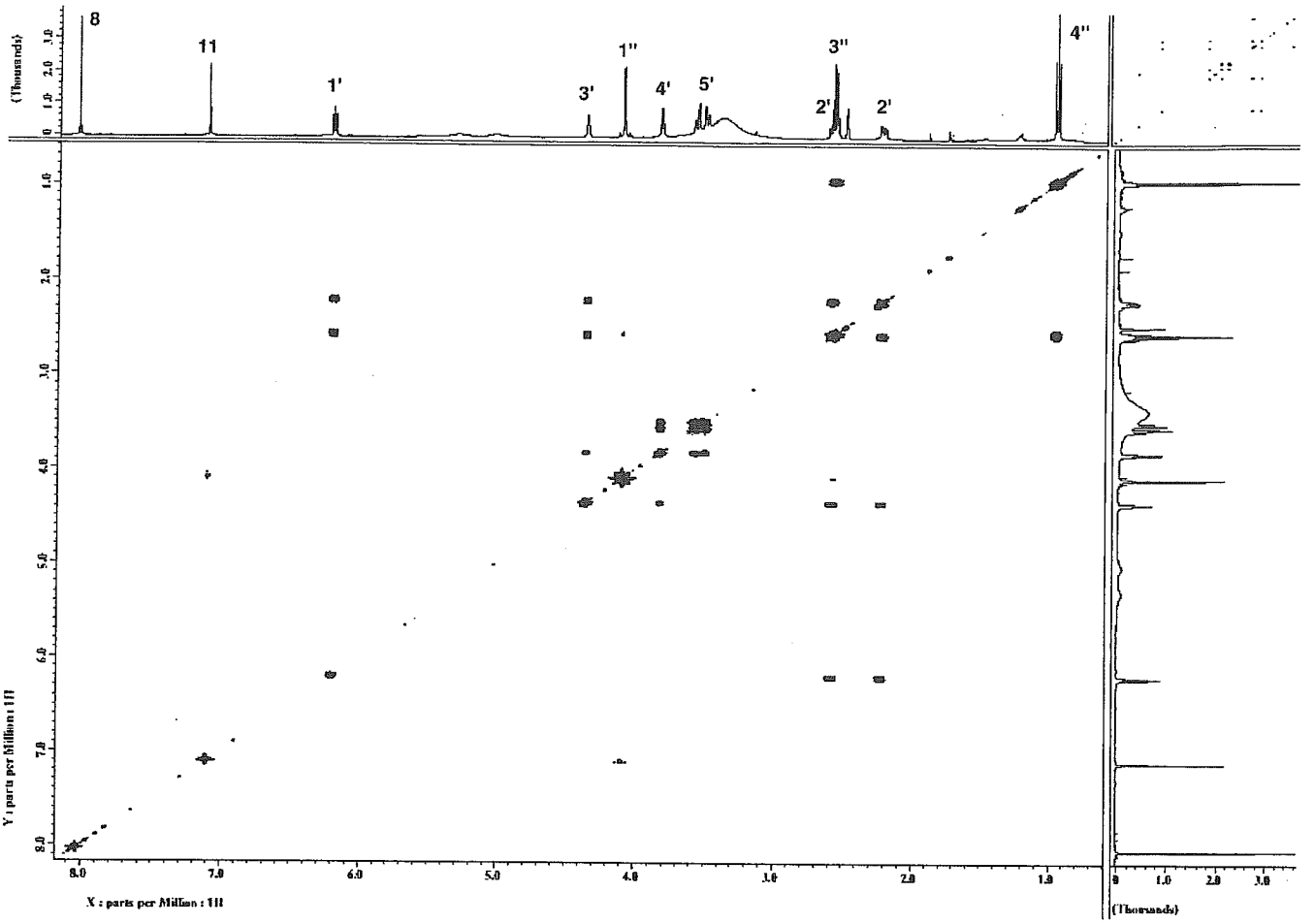

Figure 6. $^1H-^1H$ 2D COSY NMR spectrum of compound **6**.

Adduct 3 was characterized as 8-OH-dGuo, based on its two unique maxima (245 and 293 nm) in the UV spectrum (Figure 2A-3) and a comparison of its retention time in HPLC with that of authentic 8-OH-dGuo (*16*, *17*).

The mass spectra of adducts 4 and 5, $(M - H)^-$, *m/z* 352.1248 and 352.1258 (352.1257 calcd for $C_{14}H_{18}N_5O_6$), revealed an increase of 86 mass units ($C_4H_6O_2$) from dGuo. In the ^1H NMR spectrum, the presence of an ethyl group and a hemiaminal proton was observed, suggesting that they are 1,N2-cyclic ethylglyoxal-dGuo adducts. Their UV spectra (Figure 2B-4,5) are similar to those of methylglyoxal-dGuo adducts (*21*). They may be stereoisomers, because their mass, ^1H NMR, and UV spectra (Figure 2B-4,5) are identical. However, the structures of **4** and **5** were not confirmed unambiguously in the present study, because ethylglyoxal was not available.

The mass spectra of adduct 6 showed a $(M - H)^-$ ion at *m/z* 360.1308 (360.1308 calcd for $C_{16}H_{18}N_5O_5$), which corresponds to an increase of 94 mass units (C_6H_6O) from dGuo. In the ^1H NMR spectrum, the presence of an ethyl group (0.96 and 2.57 ppm), a low field methylene group (4.09 ppm), and an extra olefinic proton (7.11 ppm) was observed, in addition to the signals of the dGuo moiety. The UV spectrum of adduct 6 [λ_{max} (pH 7), 228 and 282 nm] was similar to that of 1,N2-etheno-dGuo [λ_{max} (pH 7), 228 and 283 nm], but different from that of 3,N2-ethenoguanosine [λ_{max} (pH 7), 225 and 258 nm] (*22*, *23*). The stability of the glycosyl bond of adduct 6, under conditions of 0.1% acetic acid (pH 3.2), 37 °C, and 1 h, also ruled out the possibility of the 3,N2-etheno-dGuo derivative, which is known to be rapidly hydrolyzed (half-life of 1 h) under conditions of pH 5.5, 37 °C, and 1 h (*24*). The structure of adduct 6 was proposed as a 4-oxo-2-hexenal (4-OHE)-1,N2-cyclic-dGuo adduct (structure **6**), based on these spectral data. The ^1H NMR and UV data of compound **6**, as well as the retention time in HPLC, were completely identical to those of the sole reaction product of dGuo and 4-OHE. The structure of compound **6** was confirmed by extensive NMR experiments, including COSY

Table 2. ^{13}C and ^1H NMR Assignments for Compound 6[a]

	δC (ppm)	δH (ppm)	multiplicity	*J* (Hz)
1N				
2	146.94			
3N				
4	149.79			
5	115.83			
6	153.74			
7N				
8	136.83	8.04	s	
9N				
10	117.67			
11	116.05	7.11	s	
12N				
1′	83.01	6.21	dd	7.6, 6.1
2′	39.42	2.23	ddd	13.1, 6.1, 3.1
		2.59	m	
3′	70.74	4.36	ddd	5.6, 3.1, 2.8
4′	87.64	3.83	ddd	4.7, 4.4, 2.8
5′	61.72	3.51	dd	11.7, 4.4
		3.57	dd	11.7, 4.7
3′OH				
5′OH				
1″	39.3	4.08	d	8.0
		4.11	d	8.0
2″	206.14			
3″	34.35	2.57	q	7.3
4″	7.58	0.96	t	7.3

[a] 1′−5′, numbering of sugar carbons.

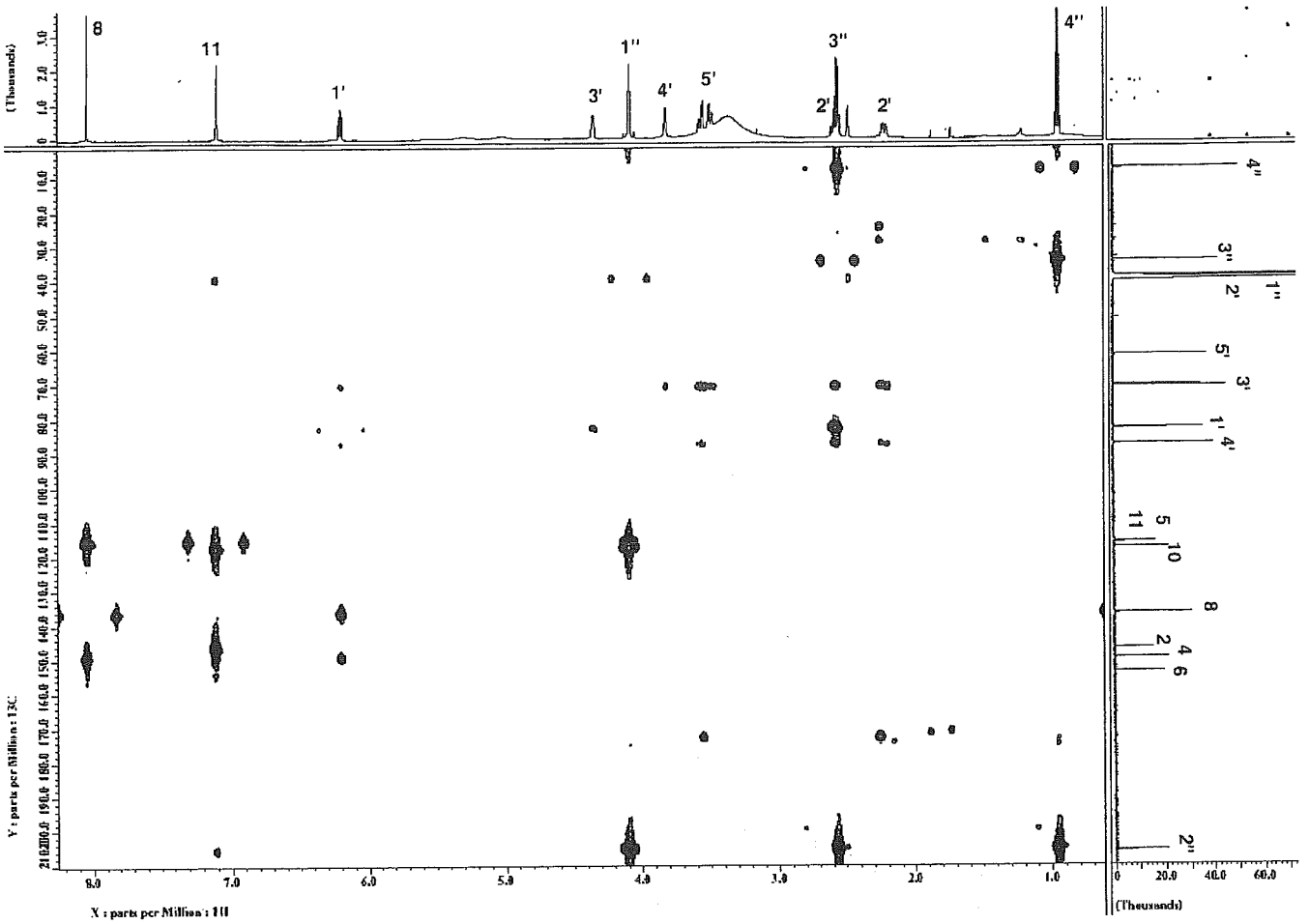

Figure 7. $^{1}H-^{13}C$ 2D HMBC NMR spectrum of compound **6**.

and HMBC, using the synthetic **6** (Table 2 and Figures 6 and 7).

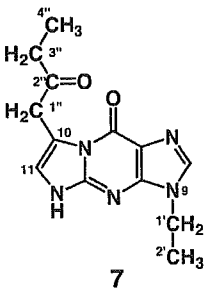

7

To further confirm its structure, a highly crystalline product, 9-ethyl-10-(2-oxobutyl)-1,N2-ethenoguanine (structure **7**), was prepared from 9-ethylguanine and 4-OHE, under the same reaction conditions used for the preparation of 10-(2-oxobutyl)-1,N2-etheno-dGuo (compound **6**). Structure **7** was analyzed by X-ray crystallography (Figure 8). Because the UV spectra and the low-field ^{1}H NMR data of **6** and **7** (Tables 2 and 3) are similar, the structure of **6** is presumed to have the same ring system and substitution pattern as those of **7**.

Mutagenic Activity of 4-OHE in *Salmonella* Strains, TA100 and TA104. The mutagenicity of 4-OHE was tested at concentrations of 1.25, 2.5, 5, 7.5, and 10 μg/plate. At concentrations above 10 μg/plate, 4-OHE was quite toxic to the bacteria. 4-OHE showed mutagenic activity in the TA100 and TA104 strains, without S9 mix (Figure 9A,B, respectively). The specific mutagenic activities of 4-OHE to TA100

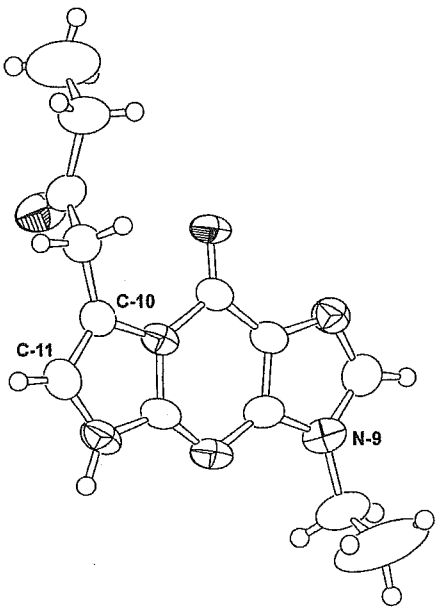

Figure 8. Crystal structure of compound **7**.

and TA104 were 78 and 67 revertants/μg, calculated from the data at the concentrations of 10 and 2.5 μg/plate, respectively. The mutagenicity of 4-OHE is also shown as the mutation frequency (revertants/ survivals) in Figure 9. 4-OHE caused a dose-dependent increase in mutation frequency in TA100 and TA104.

Table 3. ^{13}C and ^{1}H NMR Assignments for Compound 7

	δC (ppm)	δH (ppm)	multiplicity	*J* (Hz)
1N				
2	147.1			
3N				
4	150.0			
5	115.7			
6	153.8			
7N				
8	138.4	7.84	s	
9N				
10	117.5			
11	115.8	7.09	s	
12N				
1′	37.8	4.05	q	7.2
2′	15.1	1.36	t	7.2
1″	39.3	4.09	s	
2″	206.1			
3″	34.3	2.57	q	7.2
4″	7.5	0.96	t	7.2

Discussion

It is important to identify mutagens in the diet, as a prelude to cancer prevention. However, few mutagens have been identified in the human diet. It is difficult to isolate very small amounts of mutagens by HPLC from a complex mixture of chemicals, such as food, by monitoring the mutagenic activity of each fraction. For this purpose, it is more efficient to study model systems of lipid peroxidation, which may be related to high-fat and red meat diets.

In our study, the unstable mutagens present in minor amounts in the complicated mixtures of the model reactions were trapped as dGuo adducts (*16*). This method allowed us to identify mutagens, such as glyoxal, glyoxylic acid, ethylglyoxal, and 4-OHE, in the mixture. Among them, ethylglyoxal and 4-OHE have not previously been reported as mutagens.

The mutagenicity of glyoxal and methylglyoxal and their detection in various foods has been reported (*25*, *26*). Although the tumor promotion activity of glyoxal has been observed in an MNNG plus NaCl-induced stomach carcinogenesis model, glyoxal and methylglyoxal do not seem to be carcinogenic in F344 rat liver, based on a medium-term liver bioassay measuring the induction of glutathione S-transferase placental form (GST-P)-positive foci (*27*).

The mutagenicity of glyoxylic acid has also been reported as a component of an ozonated humic substance (*28*, *29*). However, its formation by lipid peroxidation has not been described. Further studies on its detection in unsaturated fatty acid-containing foods and its carcinogenicity are needed.

We detected 8-OH-dGuo in the dGuo-lipid peroxidation reaction mixture. This result is compatible with the previous observation that 8-OH-dGuo is formed from dGuo or in DNA after a reaction with autoxidized polyunsaturated fatty acids (*30*, *31*). The reason for the higher formation of 8-OH-dGuo in the MLA reaction as compared to the MLN reaction in the present study is not clear.

4-OHE may be produced via 16-hydroperoxy compound formed from MLN, followed by heme Fe-mediated decomposition, as shown in Scheme 1, by a mechanism similar to that for the formation of 4-oxo-2-nonenal (4-ONE) from 13-hydroperoxy-9,11-octadecadienoic acid (*32*). The yields of 4-OHE in the salad oil reaction (Figure 1B) and the MLN reaction (Figure 1C) from 1 mL of the corresponding oils were estimated as 12.4 and 25.8 μg, respectively, based on the peak areas of adduct 6.

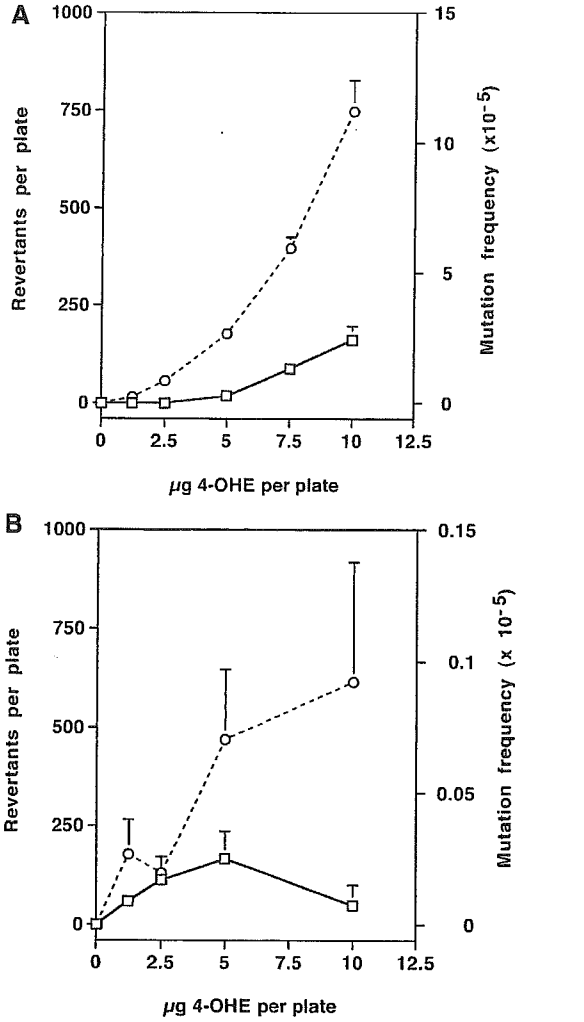

Figure 9. Mutagenicity of 4-OHE in TA100 (A) and TA104 (B). Mutagenicity (revertants/plate, —) and mutation frequency (revertants/survivals, - - -) are shown. Values represent means ± SE; $n = 4$. The number of spontaneous revertants per plate was subtracted.

Scheme 1. Mechanism for the Formation of 4-OHE from MLN

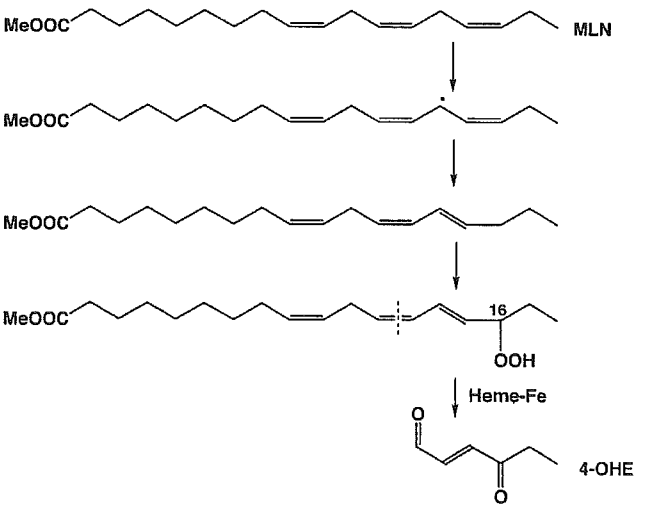

4-Hydroxy-2-nonenal and 4-ONE have been extensively studied by many researchers as the lipid peroxidation products of ω-6 fatty acids, such as linoleic acid (*32*). The structure of a 4-ONE-dGuo adduct and its detection in liver DNA from oxidative stress-induced rats have been reported (*33*, *34*). On the other hand, ω-3 fatty acids, such as α-linolenic acid,

docosahexaenoic acid (DHA), and eicosapentaenoic acid (EPA), are known as important fatty acids recommended for cancer prevention, but their lipid peroxidation products, such as 4-hydroxy-2-hexenal (*35*) and 4-OHE, have not been well-studied.

The autoxidation reaction mixture (dGuo + MLN + hemin) produced more kinds and higher amounts of dGuo adducts (Figure 1C) than the (dGuo + MLA + hemin) reaction mixture (Figure 1A). This is compatible with the fact that the autoxidation rate of unsaturated fatty acids is dependent on the number of active methylene groups between the two double bonds (*36*). Therefore, more mutagens are expected to be produced by autoxidation, in the order linoleic acid < α-linolenic acid < DHA < EPA, which have two, three, four, and five active methylene groups, respectively. The different affinities of these unsaturated fatty acids for the hemin molecule may also influence the autoxidation rate. Our data are compatible with the observation that the mutagenicity of heated cooking oils correlates with the α-linolenic acid content as reported by Harris and his collaborators (*37*). We also detected a considerable amount of 4-OHE in heat-processed ω-3 fat-containing foods, such as broiled fish and perilla oil, while the amounts of 4-ONE were much lower than those of 4-OHE (Kawai et al., to be published elsewhere). In the HPLC profile of the MLA reaction mixture (Figure 1A), we could not detect an etheno-dGuo type adduct derived from 4-ONE, even after prolonged elution with an increasing acetonitrile gradient. However, we cannot rule out the possiblity that the formation of 4-ONE-dGuo adduct has not been detected, because it may be present in oil layer in the model reaction mixtures, due to its hydrophobicity.

In addition to DNA components, 4-OHE may also react with Arg, His, and Lys residues in proteins, as 4-ONE does (*38*). These modifications may exert epigenetic effects, such as modulation of transcriptional activation (*38*) or other deleterious biological phenomena. Finally, it is worth mentioning that 4-OHE has been detected as a major constituent of insect defensive secretions, which function as nonspecific irritants, toxins, or olfactory repellents of arthropods (*39*). Our results raise the concern that ω-3 fats are more toxic than ω-6 fats, in that ω-3 fats produce larger amounts of mutagens by lipid peroxidation, even if ω-3 fats themselves in the diet inhibit carcinogenesis. Further studies on the detection of glyoxylic acid, ethylglyoxal, and 4-OHE in various foods and on the carcinogenic activity of 4-OHE are now in progress in our laboratory.

Acknowledgment. We thank Dr. K. Matsuno of the Bioinformation Research Center of our University for the measurement of mass spectra. We also thank Dr. T. Nohmi of the National Institute of Health Sciences, Japan, for providing the TA104 strain. This work was supported in part by a Grant-in-Aid for Cancer Research from the Ministry of Health, Labor, and Welfare.

References

(1) Carroll, K. K., and Braden, L. M. (1984) Dietary fat and mammary carcinogenesis. *Nutr. Cancer 6*, 254−259.

(2) Gallagher, R. P., and Kutynec, C. L. (1997) Diet, micronutrients and prostate cancer: Review of the evidence. *Can. J. Urol. 4*, 22−27.

(3) Giovannucci, E., Rimm, E. B., Stampfer, M. J., Colditz, G. A., Ascherio, A., and Willett, W. C. (1994) Intake of fat, meat, and fiber in relation to risk of colon cancer in men. *Cancer Res. 54*, 2390−2397.

(4) Potter, J. D. (1996) Nutrition and colorectal cancer. *Cancer Causes Control 7*, 127−146.

(5) Brink, M., Weijenberg, M. P., De Goeij, A. F., Schouten, L. J., Koedijk, F. D., Roemen, G. M., Lentjes, M. H., De Bruine, A. P., Goldbohm, R. A., and Van Den Brandt, P. A. (2004) Fat and K-ras mutations in sporadic colorectal cancer in The Netherlands cohort study. *Carcinogenesis 25*, 1619−1628.

(6) Sawa, T., Akaike, T., Kida, K., Fukushima, U., Takagi, K., and Maeda, H. (1998) Lipid peroxyl radicals from oxidized oils and heme-iron: Implication of high-fat diet in colon carcinogenesis. *Cancer Epidemiol. Biomarkers Prev. 7*, 1007−1012.

(7) Young, G. P., St. John, D. J. B., Rose, I. S., and Blake, D. (1990) Haem in the gut. Part II. Faecal excretion of haem and haem-derived porphyrins and their detection. *J. Gastroenterol. Hepatol. 5*, 194−203.

(8) Edionwe, A. O., and Kies, C. (2001) Comparison of palm and mixtures of refined palm and soybean oils on serum lipids and fecal fat and fatty acid excretions of adult humans. *Plant Foods Hum. Nutr. 56*, 157−165.

(9) Burcham, C. B. (1999) Internal hazards: Baseline DNA damage by endogenous products of normal metabolism. *Mutat. Res. 443*, 11−36.

(10) Marnett, L. J., Hurd, H. K., Hollstein, M. C., Levin, D. E., Esterbauer, H., and Ames, B. N. (1985) Naturally occurring carbonyl compounds are mutagens in Salmonella tester strain TA104. *Mutat. Res. 148*, 25−34.

(11) Feng, Z., Hu, W., Amin, S., and Tang, M. S. (2003) Mutational spectrum and genotoxicity of the major lipid peroxidation product, *trans*-4-hydroxy-2-nonenal, induced DNA adducts in nucleotide excision repair-proficient and -deficient human cells. *Biochemistry 42*, 7848−7854.

(12) Esterbauer, H., and Weger, W. (1967) Uber die wirkungen von aldehyden auf gesunde und maligne zellen 3. Mitt: Synthese von homologen 4-hydroxy-2-alkenalen, II. *Monatsh. Chem. 98*, 1994−2000.

(13) Altomare, A., Burla, M. C., Camalli, M., Cascarano, M., Giacovazzo, C., Guagliardi, A., and Polidori, G. (1994) *J. Appl. Crystallogr. 27*, 435.

(14) Beurskens, P. T., Admiraal, G., Beurskens, G., Bosman, W. P., de Gelder, R., Israel, R., and Smits, J. M. M. (1994) The DIRDIF-94 program system, Technical Report of the Crystallography Laboratory, University of Nijmegen, The Netherlands.

(15) Maron, D. M., and Ames, B. N. (1983) Revised methods for the Salmonella mutagenicity test. *Mutat. Res. 113*, 173−215.

(16) Kasai, H., Hayami, H., Yamaizumi, Z., Saito, H., and Nishimura, S. (1984) Detection and identification of mutagens and carcinogens as their adducts with guanosine derivatives. *Nucleic Acids Res. 12*, 2127−2136.

(17) Kasai, H., and Nishimura, S. (1984) Hydroxylation of deoxyguanosine at C-8 position by ascorbic acid and other reducing agents. *Nucleic Acids Res. 12*, 2137−2145.

(18) Staehelin, M. (1959) Inactivation of virus nucleic acid with glyoxal derivatives. *Biochim. Biophys. Acta 31*, 448−454.

(19) Shapiro, R., and Hachmann, J. (1966) The reaction of guanine derivatives with 1,2-dicarbonyl compounds. *Biochemistry 5*, 2799−2807.

(20) Kasai, H., Iwamoto-Tanaka, N., and Fukada, S. (1998) DNA modifications by the mutagen glyoxal: Adduction to G and C, deamination of C and GC and GA cross-linking. *Carcinogenesis 19*, 1459−1465.

(21) Vaca, C. E., Fang J. L., Conradi, M., and Hou, S. M. (1994) Development of a ^{32}P-postlabeling method for the analysis of 2′-deoxyguanosine-3′-monophosphate and DNA adducts of methylglyoxal. *Carcinogenesis 15*, 1887−1894.

(22) Sodum, R. S., and Chung, F.-L. (1988) 1,N2-Ethenodeoxyguanosine as a potential marker for DNA adduct formation by *trans*-4-hydroxy-2-nonenal. *Cancer Res. 48*, 320−323.

(23) Kusmierek, J. T., Jensen, D. E., Spengler, S. J., Stolarski, R., and Singer, B. (1987) Synthesis and properties of N2,3-ethenoguanosine and N2,3-ethenoguanosine 5′-diphosphate. *J. Org. Chem. 52*, 2374−2378.

(24) Kusmierek, J. T., Folkman, W., and Singer, B. (1989) Synthesis of N2,3-ethenodeoxyguanosine, N2,3-ethenodeoxyguanosine 5′-phosphate, and N2,3-ethenodeoxyguanosine 5′-triphosphate. Stability of the glycosyl bond in the monomer and in poly(dG,ϵdG-dC). *Chem. Res. Toxicol 2*, 230−233.

(25) Kasai, H., Kumeno, K., Yamaizumi, Z., Nishimura, S., Nagao, M., Fujita, Y., Sugimura, T., Nukaya, H., and Kosuge, T. (1982) Mutagenicity of methylglyoxal in coffee. *Gann. 73*, 681−683.

(26) Nagao, M., Fujita, Y., Sugimura, T., and Kosuge, T. (1986) Methylglyoxal in beverages and foods: Its mutagenicity and carcinogenicity. *IARC Sci. Publ. 70*, 283−291.

(27) Hasegawa, R., Ogiso, T., Imaida, K., Shirai, T., and Ito, N. (1995) Analysis of the potential carcinogenicity of coffee and its related compounds in a medium-term liver bioassay of rats. *Food Chem. Toxicol. 33*, 15−20.

(28) Sayato, Y., Nakamuro, K., and Ueno, H. (1987) Mutagenicty of products formed by ozonation of naphthoresorcinol in aqueous solutions. *Mutat. Res. 189*, 217−222.

(29) Matsuda, H., Ose, Y., Sato, T., Nagase, H., Kito, H., and Sumida, K. (1992) Mutagenicity from ozonation of humic substances. *Sci. Total Environ. 30*, 117−118, 521−529.

(30) Kasai, H., and Nishimura, S. (1989) Formation of 8-hydroxydeoxyguanosine in DNA by auto-oxidized unsaturated fatty acids. In *Medical, Biological and Chemical Aspects of Free Radical Research* (Hayaishi, et al., Eds.) pp 1021−1023, Elsevier Science Publishers B. V., Amsterdam.

(31) Park, J.-W., and Floyd, R. A. (1992) Lipid peroxidation products mediate the formation of 8-hydroxydeoxyguanosine in DNA. *Free Radical Biol. Med. 12*, 245−250.

(32) Lee, S. H., and Blair, I. A. (2000) Characterization of 4-oxo-2-nonenal as a novel product of lipid peroxidation. *Chem. Res. Toxicol. 13*, 698−702.

(33) Rindgen, D., Nakajima, M., Wehrli, S., Xu, K., and Blair, I. A. (1999) Covalent modifications to 2′-deoxyguanosine by 4-oxo-2-nonenal, a novel product of lipid peroxidation. *Chem. Res. Toxicol. 12*, 1195−1204.

(34) Kawai, Y., Kato, Y., Nakae, D., Kusuoka, O., Konishi, Y., Uchida, K., and Osawa, T. (2002) Immunohistochemical detection of substituted 1,N2-ethenodeoxyguanosine adduct by ω-6 polyunsaturated fatty acid hydroperoxides in the liver of rats fed a choline-deficient L-amino acid-defined diet. *Carcinogenesis 23*, 485−489.

(35) Van Kuijk, F. J. G. M., Holte, L. L., and Dratz, E. A. (1990) 4-Hydroxyhexenal: A lipid peroxidation product derived from oxidized docosahexaenoic acid. *Biochem. Biophys. Acta 1043*, 116−118.

(36) Cosgrove, J. P., Church, D. F., and Pryor, W. A. (1987) The kinetics of the autoxidation of polyunsaturated fatty acids. *Lipids 22*, 299−304.

(37) Shields, P. G., Xu, G. X., Blot, W. J., Fraumeni, J. F., Jr., Trivers, G. E., Pellizzari, E. D., Qu, Y. H., Gao, Y. T., and Harris, C. C. (1995) Mutagens from heated Chinese and U.S. cooking oils *J. Natl. Cancer Inst. 87*, 836−841.

(38) Oe, T., Arora, J. S., Lee, S. H., and Blair, I. A. (2003) A novel lipid hydroperoxide-derived cyclic covalent modification to histone H4. *J. Biol. Chem. 278*, 42098−42105.

(39) Williams, L., 3rd, Evans, P. E., and Bowers, W. S. (2001) Defensive chemistry of an aposematic bug, Pachycoris stallii Uhler and volatile compounds of its host plant Croton californicus Muell.-Arg. *J. Chem. Ecol. 27*, 203−216.

TX050236M

Industrial Health 2005, 43, 699–701 Short Communication

4-Oxo-2-hexenal, a Mutagen Formed by ω-3 Fat Peroxidation, Causes DNA Adduct Formation in Mouse Organs

Hiroshi KASAI[1] *, Muneyuki MAEKAWA[1, 2], Kazuaki KAWAI[1], Kenji HACHISUKA[2], Yoshikazu TAKAHASHI[3], Hikaru NAKAMURA[3], Ryuichi SAWA[3], Saburo MATSUI[4] and Tomonari MATSUDA[4]

[1] Department of Environmental Oncology, Institute of Industrial Ecological Sciences;
[2] Department of Rehabilitation Medicine; University of Occupational and Environmental Health, 1-1 Iseigaoka, Yahatanishi-ku, Kitakyushu 807-8555, Japan
[3] Microbial Chemistry Research Center, 3-14-23, Kamiosaki, Shinagawa-ku, Tokyo 141-0021, Japan
[4] Department of Technology and Ecology, Graduate School of Global Environmental Studies, Kyoto University, Sakyo, Kyoto 606-8501, Japan

Received March 28, 2005 and accepted August 29, 2005

Abstract: To identify mutagens formed in a model reaction of lipid peroxidation, linolenic acid methyl ester and hemin were reacted with dG. As a result, a 4-oxo-2-hexenal-dG adduct (dG*) was identified in the model reaction mixture. The 4-oxo-2-hexenal (4-OHE) showed mutagenic activity in the Salmonella typhimurium strains TA100 and TA104. After 4-OHE was orally administered to mice, dG*, 4-OHE-dC- and 4-OHE-5-methyl-dC adducts were detected in esophageal, stomach and intestinal DNA. In the vapor phase released from the methyl linolenate-hemin model system, and in the smoke released during the broiling of fish, 4-OHE was detected by GCMS. The 4-OHE seems to be produced by the auto-oxidation of ω-3 polyunsaturated fatty acids. These results provide a warning to workers dealing with ω-3 fats, who may be exposed to this volatile mutagen.

Key words: 4-oxo-2-hexenal, ω-3 polyunsaturated fatty acids, DNA adduct

It is important to identify environmental mutagens and to remove them to prevent cancer in industry workers. We have been interested in the mutagens produced by lipid peroxidation[1, 2], because they may be formed during the extraction and purification of edible oils, or by frying foods with vegetable-oil. Many low molecular-weight mutagens are released into the atmosphere by oil factories, the food industry, and restaurant kitchens. Various lipid peroxide compounds are produced by the oxidative fragmentation of fats catalyzed by iron and heat or light. Our study focused on the identification of mutagens in the lipid peroxide products formed from ω-3 polyunsaturated fatty acids, such as linolenic acid.

It is well known that many mutagens react with DNA components, particularly with deoxyguanosine (dG)[3]. To identify the mutagens formed in a model reaction of lipid peroxidation, linolenic acid methyl ester and hemin were reacted with dG in phosphate buffer (pH 7.4), as an emulsion for 72 h at 20°C. The dG-mutagen adducts were isolated by HPLC, and their structures were determined by mass-, UV-, ^{1}H- and ^{13}C-NMR spectra. As a result, the 4-oxo-2-hexenal-dG adduct (dG*) was identified in the model reaction mixture. M+Na, m/e 384.1256 (384.1284 calcd. for $C_{16}H_{19}N_5NaO_5$); UV λmax in H_2O, 228, 280 nm. The structure was confirmed by comparison with an authentic dG* sample prepared from synthetic 4-oxo-2-hexenal (4-

*To whom correspondence should be addressed.

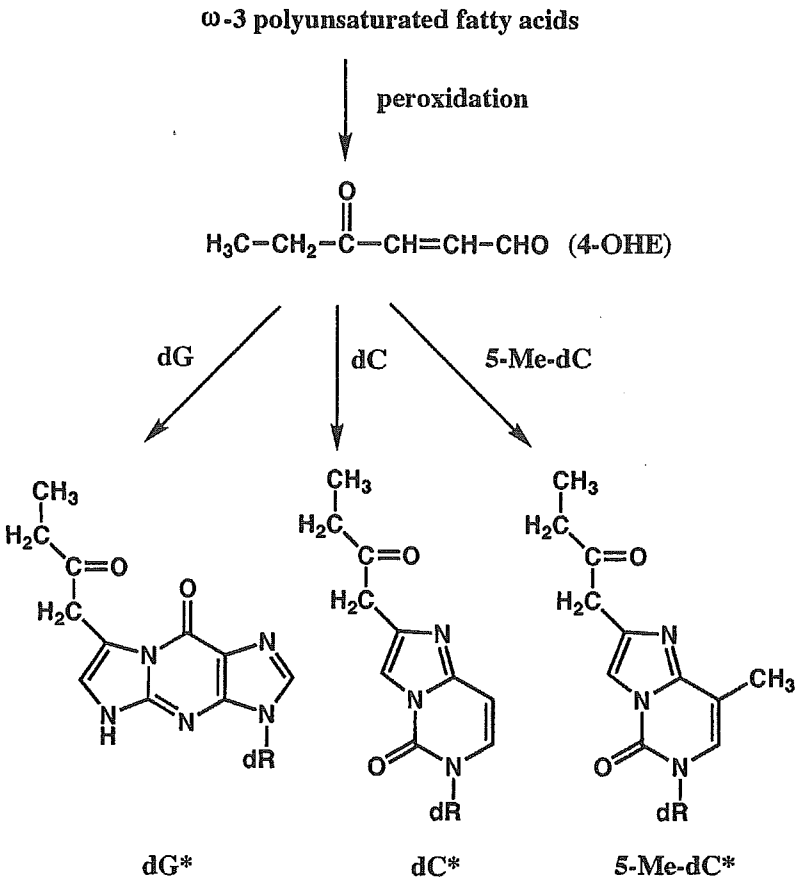

Fig. 1. Structures of DNA adducts formed by 4-oxo-2-hexenal.

OHE) and dG, and by X-ray crystallography of the 4-OHE-9-ethylguanine-adduct. The 4-OHE was mutagenic in the Salmonella strains, TA100 and TA104, without S9 mix. Its specific mutagenic activities against TA100 and TA104 were 78 and 67 revertants/μg, respectively. The mutagenicity of 4-OHE has not been reported thus far. It also induced apoptosis in human HL-60 cells. This is reasonable because DNA damage is a common trigger for apoptosis induction in mammalian cells[4].

The 4-OHE reacts not only with dG but also with dC and 5-methyl-dC to yield adducts (dG*, dC*, 5-methyl-dC*). The structures of dC*and 5-methyl-dC* were determined mainly by mass-, ^{1}H- and ^{13}C-NMR- spectra. dC*: M+Na, m/e 344.1192 (344.1222 calcd. for $C_{15}H_{19}N_3NaO_5$); UV λmax in H_2O, 227 nm. 5-methyl-dC*: M+Na, m/e 358.1372 (358.1379 calcd. for $C_{16}H_{21}N_3NaO_5$); UV λmax in H_2O, 278 nm. The structure of dC* was confirmed by X-ray crystallography. After the reaction of 4-OHE with double stranded calf thymus DNA, the yield of these DNA modifications were dC* > 5-methyl-dC* > dG*. The more efficient formation of dC* than dG* in DNA may be due to the fact that the amino group of dC in DNA is located in the major groove, while that of dG is in the minor groove and is more sterically hindered. As a prelude for testing its genotoxicity *in vivo*, 4-OHE (3 mg) was orally administered to mice, and after 24 h, the DNA was isolated from the esophagus, stomach, intestine, liver and kidney. The DNA was enzymatically digested to deoxynucleosides, and was subjected to LC/MS/MS analyses. Particularly, in the esophagus, stomach and intestine DNA, dC* was detected in the range of 2.0, 5.5 and 1.1 adducts / 10^7 dC, respectively. Lower amounts of 5-methyl-dC* and dG* were also detected in these organ DNAs.

It is important to confirm the formation of 4-OHE in a model system of lipid peroxidation, as well as during the heat processing of edible vegetable oil, and during cooking. From ethylacetate traps (extracts) of the vapor phase released from the heated methyl linolenate-hemin model system, and the smoke released during the broiling of fish, 4-OHE was detected by GCMS. Commercial perilla oil, which is rich in linolenic acid (40–50 μg/g), the edible part of broiled fish (5–170 μg/g), and various fried foods (5–50 μg/g) also

contained high levels of 4-OHE. It was present at an especially high concentration (70–170 μg/g) in broiled saury. However, 4-oxo-2-nonenal[5], a cognate longer carbon chain derivative, was only detected in an one order of magnitude lower range in these food products. This may be due to the fact that the major natural ω-3 polyunsaturated fatty acids, such as linolenic acid, DHA and EPA, the precurser of 4-OHE, are more easily oxidized than ω-6 fatty acids, such as linoleic acid.

Workers involved in the manufacturing of vegetable oils, such as colza oil and soybean oil, which contain linolenic acid, will be exposed to 4-OHE during the crude oil extraction and purification. The same is true for workers manufacturing instant cup noodles and snack foods, and producing EPA and DHA from fish oil. Kitchen workers involved in frying foods or broiling fish in restaurants may also be exposed to 4-OHE. Since 4-OHE induces DNA adduct formation in experimental animal organs, it is possible that 4-OHE is an important human carcinogen. Further studies on the carcinogenicity of 4-OHE and its detection in working environments will be required.

Acknowledgement

We would like to thank Dr. T. Nohmi of the National Institute of Health Sciences, Tokyo, for providing us the S. typhimurium strains for the mutagenicity test.

References

1) Esterbauer H, Schaur, RJ, Zollner H (1991) Chemistry and biochemistry of 4-hydroxynonenal, malonaldehyde and related aldehydes. Free Radical Biol Med **11**, 81–128.
2) Horton AA, Fairhurst S (1987) Lipid peroxidation and mechanisms of toxicity. Crit Rev Toxicol **18**, 27–79.
3) Kasai H, Hayami H, Yamaizumi Z, Saito H, Nishimura S (1984) Detection and identification of mutagens and carcinogens as their adducts with guanosine derivatives. Nucl Acids Res **12**, 2127–36.
4) Narbury CJ, Zhivotovsky B (2004) DNA damage-induced apoptosis. Oncogene **23**, 2797–808.
5) Lee SH, Blair IA (2000) Characterization of 4-oxo-2-nonenal as a novel product of lipid peroxidation. Chem Res Toxicol **13**, 698–702.

Pathology International 2006; **56**: 117–125 doi:10.1111/j.1440-1827.2006.01940.x

Original Article

Chromosomal numerical abnormalities in early stage lung adenocarcinoma

Takehisa Sano,[1] Yasuhiko Kitayama,[1] Hisaki Igarashi,[1] Masaya Suzuki,[1] Fumihiko Tanioka,[1,3] Kingo Chida,[2] Koji Okudela[1] and Haruhiko Sugimura[1]

Departments of [1]Pathology and [2]Internal Medicine, Hamamatsu University School of Medicine, Hamamatsu and [3]Department of Pathology, Iwata City Hospital, Iwata, Japan

Chromosomal numerical abnormalities (CNA) are ubiquitous in human cancers. However, the question of when a CNA occurs in the course of tumor generation and progression, is controversial. Recent radiological scrutiny has enabled the identification of small peripheral lesions in the lung. A chromosome-wide investigation encompassing almost all the chromosomal centromeres was performed using modified fluorescence *in situ* hybridization on the archived pathological samples of 16 atypical adenomatous hyperplasia (AAH) and 30 lung adenocarcioma (AdCa) specimens including those smaller than 1 cm in size. The prevalence of the gain was more extensive in male than in female patients, and in non-smokers than in smokers. It tended to be greater in poorly differentiated AdCa, in moderately differentiated AdCa, and in well-differentiated AdCa cases, in that order. Most AAH had non-specific gains affecting all the examined chromosomes. The prevalence of the gain differed significantly between AAH and bronchioloalveolar carcinoma (BAC) ≤ 1 cm, but not between BAC < 1 cm and well-differentiated AdCa > 1 cm. It is proposed that the CNA is a distinct phenomenon occurring in the early or premalignant stage of lung AdCa, and that the CNA itself may not be a sequel in the carcinogenetic process, but a driving factor in carcinogenesis.

Key words: adenocarcinoma, adenomatous hyperplasia, aneuploidy, chromosomal numerical abnormality, fluorescence *in situ* hybridization, lung cancer

The processes of tumorigenesis have been assumed to be driven by the progressive accumulation of somatic mutations in a number of genes,[1] and genomic instability is proposed to be a driving force in the initiation of tumorigenesis.[2,3] Recent studies suggest that a chromosomal numerical abnormality (CNA) may also contribute to tumorigenesis,[4–8] but controversy exists as to whether the CNA is involved in tumor generation, initiation, and progression or is a simple consequence of multiple genetic events.[9,10]

CNA are a well-known characteristic of lung cancer as well as of other cancers. So far, few studies investigated numerical chromosome alterations genome-wide using centromeric α-satellite probes by fluorescence *in situ* hybridization (FISH) in non-small cell lung cancer (NSCLC).[11] Our knowledge of CNA in NSCLC thus remains limited, and is almost nonexistent except for one anecdotal report concerning the putative premalignant lesion, atypical adenomatous hyperplasia (AAH).[12] Recent genome-wide approaches such as comparative genomic hybridization (CGH) and oligonucleotide microarray are revealing extensive alterations, both genetic gain and loss in tumors, but still an artificial genomic amplification is necessary to obtain the changes in a small amount of DNA such as that from small lesions. In recent debates about the roles of aneuploidy and mutations concomitant with the origin of human cancer, it is important to know how extensively the CNA is present in lung carcinogenesis, that is, in AAH and small adenocarcinomas (AdCa) without metastasis. In this report we took advantage of a modified FISH protocol for pathology archives (in which the investigation of the CNA profile is difficult because the tissue has previously been identified, embedded, and stored in paraffin blocks). Extensive recording of numerical centromere abnormalities in cases of AAH and AdCa of the lung, including one case of AdCa in AAH, was performed in light of the concept of a stepwise progression of lung adenocarcinoma. In order to improve specificity and sensitivity,[13,14] we used intermittent microwave irradiation (MW) in the process of *in situ* hybridization using centromere-specific α-satellite probes for 18 chromosomes.

Correspondence: Haruhiko Sugimura, MD, PhD, First Department of Pathology, Hamamatsu University School of Medicine, 1-20-1, Handayama, Hamamatsu 431-3192, Japan.
Email: hsugimur@hama-med.ac.jp

Received 19 October 2005. Accepted for publication 8 November 2005.

MATERIALS AND METHODS

Samples

All specimens in the study were obtained from pathology archives stored at Hamamatsu University Hospital and its affiliated hospitals. All the subjects from whom the specimens were taken, except three who had chest symptoms (cough, bloody sputum or chest pain), were asymptomatic and were recruited to surgery by detection of a coin lesion in chest radiographs or chest computed tomography. The characteristics of 28 AdCa patients and 14 AAH patients are summarized in Table 1. For one patient who had a pathologically heterogeneous lesion consisting of well-differentiated AdCa and poorly differentiated AdCa, we examined both portions separately. Another had spatially independent double cancers, well-differentiated AdCa in the upper lobe and bronchioloalveolar carcinoma (BAC) in the middle lobe. Furthermore, an additional two subjects had double AAH lesions at different sites. A total of 46 specimens (30 primary lung AdCa and 16 AAH) from 42 patients were investigated. In addition, one case in which BAC surrounded by AAH (Fig. 1c), was investigated in the same way. The specimens had been fixed in neutral-buffered formalin (3.6%), embedded in paraffin, and stored at room temperature for up to 11 years. The mean age of the AdCa patients was 64 years, with a male : female ratio of 0.56 and a smoker : non-smoker ratio of 0.33. The mean age of the AAH patients was 61 years, with a male : female ratio of 0.75 and a smoker : non-smoker ratio of 0.75. There was no particular difference in the profile of the two groups of patients. The clinicopathological profile of the specimens is shown in Table 1. The percentage of cases at pathological stage 1 AdCa (International Union Against Cancer, UICC)[15] was 71% (20/28). Two patients were at stage 2, and six were at stage 3; all but one of the stage 3 poorly differentiated AdCa were >1 cm in greatest dimension. All of the seven BAC, four well-differentiated AdCa, and one poorly differentiated AdCa were ≤1 cm in greatest dimension and 10 specimens >1 cm were at stage 1 (UICC).

Twelve non-tumor control samples had been taken from the non-tumorous portion of the lungs of subjects, nine of whom had pneumothorax, and three had interstitial pneumonia with severe alveolitis. We also counted two cases of non-tumor portions of lung cancer and the counting results of these two cases were not different from the other 12 specimens, but we show the results based on the calculations and countings of 12 tissues from non-cancer subjects.

Histological evaluation

AAH and BAC were defined according to the World Health Organization (WHO) criteria.[16] AdCa was classified into three

Table 1 Subject characteristics

	AAH			AdCa			
No. specimens (patients)	16 (14)			30 (28)			
Mean age (range) (years)	61 (44–76)			64 (42–84)			
Male/female	6/8			10/18			
Smoker/non-smoker	6/8			7/21			
Pathological stage (pT1/pT2/pT3)				20/2/6			
Tumor size (range) (cm)	0.5 (0.2–1.0)			1.6 (0.3–4.0)			
Pathological classification (*n*)	Low-grade (9)	High-grade (7)		Mod. diff.		Poorly diff.	
			Well-diff.				
		AdCa ≤ 1 cm	AdCa > 1 cm	AdCa > 1 cm		AdCa ≤ 1 cm	AdCa > 1 cm
		11 (BAC, 7)	7	7		2	3

AAH, atypical adenomatous hyperplasia; AdCa, adenocarcinoma; BAC, bronchioloalveolar carcinoma; diff., differentiated; mod., moderately.

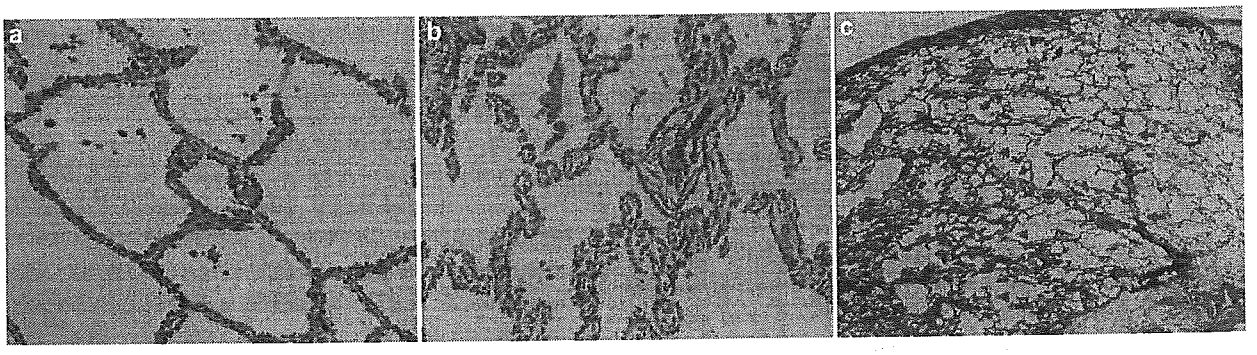

Figure 1 Hematoxylin–eosin (HE) sections of atypical adenomatous hyperplasia (AAH) and bronchioloalveolar carcinoma (BAC). (**a**) Low-grade AAH (HE; original magnification, ×200). (**b**) High-grade AAH. The prominence of alveolar cell atypism is greater than that in low-grade AAH (HE; original magnification, ×200). (**c**) BAC in high-grade AAH in the peripheral lung. The center of the lesion (arrowheads, left lower corner of the figure) shows greater atypism than the surrounding area (arrows; HE; original magnification, ×200).

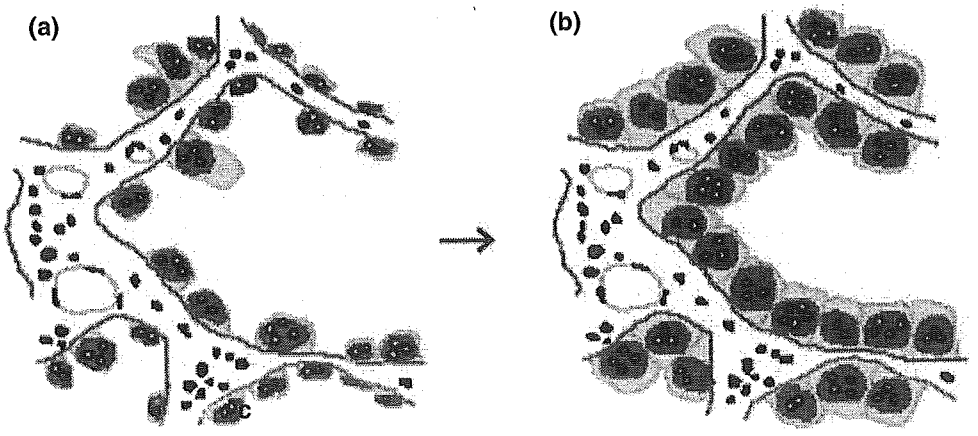

Figure 2 Stepwise chromosomal numerical abnormality (CNA) progression from (**a**) atypical adenomatous hyperplasia (AAH) to (**b**) bronchioloalveolar carcinoma (BAC). Extent of CNA (both chromosome numbers per cell and aneuploidal cell numbers) progresses from AAH to BAC, consistent with the idea of chromosomal aberration load: AAH as field cancerization has already acquired some degree of CNA. One cell (or cells) from this area may transform into a malignant cell and proliferate, resulting in BAC.

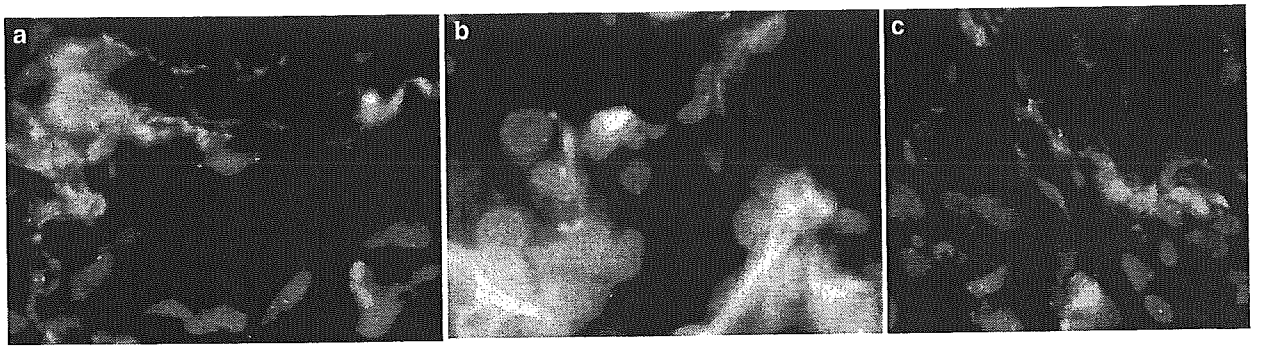

Figure 3 Fluorescence *in situ* hybridization (FISH) images of atypical adenomatous hyperplasia (AAH) and bronchioloalveolar carcinoma (BAC). (**a**) FISH in low-grade AAH: a few scattered cells with three green signals, centromere enumeration probe (CEP) 4 per nucleus (original magnification, ×600). (**b**) Dual-color FISH in high-grade AAH: cells with more than three green signals, CEP 6 and orange signals, CEP 4 exist in a group (original magnification, ×600). (**c**) Dual-color FISH in BAC: Cells with more than three green signals, CEP 17 and orange signals, CEP 3 cover a wide area (original magnification, ×600).

types according to differentiation. The grading of AAH has already been defined in published criteria.[17] According to Koga *et al.*, AAH could be classified into two grades based on histological atypia.[17] Low-grade AAH consisted of a single layer of mildly atypical uniform cells intermittently or continuously lining the alveolar septa (Fig. 1a). High-grade AAH had more increased cellularity and cellular atypia than did low-grade AAH, such as enlarged and hyperchromatic nuclei and an increased nuclear : cytoplasmic ratio (Fig. 1b). The pathological stage was determined according to the UICC tumor–node–metastasis classification.[15]

FISH with intermittent microwave irradiation

A tissue microarray with a diameter of 2–5 mm from each paraffin block of 12–25 specimens was made and was embedded in one block. A 5 μm section was put on a poly-L-lysine-coated glass slide. A panel of 18 centromeric α-satellite DNA probes (D1Z5, D2Z, D3Z1, D4Z1, D6Z1, D7Z1, D8Z2, D9Z1, D10Z1, D11Z1, D12Z3, D15Z1, D16Z1, D17Z1, D18Z1, D20Z1, DXZ1, DYZ3) derived from chromosomes 1, 2, 3, 4, 6, 7, 8, 9, 10, 11, 12, 15, 16, 17, 18, 20, X, Y, respectively, were purchased from Vysis (Downers Grove, IL, USA). All the probes were labeled either orange (Cy3) or green (fluorescein isothiocyanate (FITC)). The generalized procedure for FISH analysis consisted of sample preparation comprising denaturation, hybridization, rinsing, counterstain, and visualization. For formalin-fixed, embedded samples, however, this procedure is not enough to generate clear signals. Thus we applied intermittent MW treatment to the slides in addition to using the conventional FISH protocol.[13,14]

Counting and statistical analysis

The number of signals per cell was counted for a total of 50–100 intact and non-overlapping cell nuclei. A cell with three signals and more per nucleus was defined as gain. One or no signal per nucleus was defined as loss. As identified in the values in the control specimens shown in Tables 2,3, our method has a greater chance of wrongly finding 'loss' by missing a part of the nuclei. There is a high background, up to 20%, regarding loss of centromeres. We and the other authors had taken this limitation into account in the previous interpretation of FISH signals, that is, the cut-off had been intentionally set at a higher percentage, for example 30–40%, in defining 'loss'.

In the present report we calculated the proportion of the number of cells with altered chromosomes divided by the total number of cells. The analysis of the CNA data, when comparing sex, smoking habits, stage and histopathological types, was performed with Fisher's exact test using SAS release 9.1 (SAS Institute, Cary, USA).

In addition to this calculation, we set the cut-off based on the control specimen, then defined the cells with altered chromosomes as those outside this cut-off. One way is to calculate the mean ± 3 SD and to use this as a cut-off point. Another way is to set a cut-off point by arbitrarily taking some safety area. Many previous papers have adopted this arbi-

Table 2 Prevalence of gain

	Control (%)	a	Low-grade AAH (%)	b	High-grade AAH (%)	c	BAC < 1 cm (%)	d	AdCa < 1 cm (%)
CEP 1	1	<	10	<	16	<	32		34
CEP 2	2		4	<	10	<	22		18
CEP 3	1	<	7	<	13		17		20
CEP 4	2	<	9	<	14	<	30	>	21
CEP 6	0	<	6		9	<	23	<	34
CEP 7	0	<	9		11		13		13
CEP 8	1	<	14		12	<	26		28
CEP 9	1	<	8		12		18		19
CEP 10	1		4	<	9		14		13
CEP 11	1	<	9		13		14	>	6
CEP 12	1	<	7		7		7		7
CEP 15	1	<	10		12		16	>	4
CEP 16	0	<	8		11	<	28		35
CEP 17	1	<	10		14		18		22
CEP 18	1	<	5	<	10		12		8
CEP 20	1		3	<	9		13		10
CEP X	2	<	9	<	28		23	<	37
CEP Y	2	<	10		19	<	30		34
Average	1	<	8	<	13	<	20		21

AAH, atypical adenomatous hyperplasia; AdCa, adenocarcinoma; BAC, bronchioloalveolar carcinoma; diff, differentiated.

Mean ± SD (%) of gain of control, low-grade AAH, high-grade AHH, BAC, and AdCa: 1.006 ±0.556; 7.811 ±2.898; 12.689 ±4.827; 19.683 ±7.137; and 20.206 ±11.208, respectively.

[a,b,c,d]Fisher's exact test, $P < 0.01$; [a]<, greater in low-grade AAH; [b]<, greater in high-grade AAH; [c]<, greater in BAC < 1 cm; [d]>, greater in BAC < 1 cm, <, greater in well-diff. AdCa < 1 cm.

Table 3 Prevalence of loss

	Control (%)	a	Low-grade AAH (%)	b	High-grade AAH (%)	c	BAC < 1 cm (%)	d	AdCa < 1 cm (%)
CEP 1	28	>	18		18		20		18
CEP 2	18		18	<	25	>	13		17
CEP 3	26	>	18		18		20		18
CEP 4	22		20		18		15		18
CEP 6	29	>	21		23	>	13		12
CEP 7	22		22		19		26		23
CEP 8	20		19		18		16		17
CEP 9	20		25		27	>	17		18
CEP 10	22		22		19		15		15
CEP 11	24		22		19		20		17
CEP 12	22		20		20		23	<	34
CEP 15	24		20		17		23		29
CEP 16	19		20		16		18		18
CEP 17	27		23		23		18		21
CEP 18	20		24		21		22		17
CEP 20	19	<	31	>	20		22		23
CEP X	11	<	24	>	11		16	>	7
CEP Y	8		0		6	>	2		3
Average	21		21	>	19		18		18

AAH, atypical adenomatous hyperplasia; AdCa, adenocarcinoma; BAC, bronchioloalveolar carcinoma; diff, differentiated.

Means ± SD (%) of loss for control, low-grade AAH, high-grade AHH, BAC, and AdCa: 21.061 ±5.231; 20.350 ±5.945; 18.789 ±4.713; 17.578 ±5.393; and 17.994 ±6.997, respectively.

[a, b, c, d]Fisher's exact test: $P < 0.01$; [a]>, greater in control; <, greater in low-grade AAH; [b]>, greater in low-grade AAH; <, greater in high-grade AAH; [c]>, greater in high-grade AAH; [d]>, greater in BAC < 1 cm, <, greater in well diff. AdCa < 1 cm.

trary cut-off point.[11] Because the trend was the same (data not shown) between the three methods, we present the results using Fisher's test.

With regard to magnitude of the chromosome gains, we recorded the numbers of tumor cells having ≥5 particular chromosomes per cell.

RESULTS

Substantial CNA in AAH and stepwise addition in a transit to BAC

We succeeded in obtaining a clear signal with each centromere enumeration probe (CEP) in a total of 86% of the specimens. The subject profile is given in Tables 2,3. Gains were noted in low-grade AAH and also in all 18 chromosomes examined in high-grade AAH (Table 2). The prevalence of the gain of chromosomes 1, 2, 4, 6, 8, 16 and Y was significantly greater ($P < 0.01$) in BAC < 1 cm than in high-grade AAH. In particular, the prevalence of the gain of chromosomes 1 and 4 increased from the control to low-grade AAH, high-grade AAH, and BAC < 1 cm in this order. As to the average of the gains, it also gradually increased from the control to low-grade AAH, high-grade AAH, and BAC < 1 cm, in this order. But there was no difference between BAC < 1 cm and well-differentiated AdCa < 1 cm. Thus, our observations suggest that the gradual gain of chromosomes parallels presumable development from AAH to BAC. In contrast, it was difficult to determine any clear tendency of particular or general chromosomal loss in these early sequences (Table 3). Considering that there have been already many studies reporting loss of heterozygosity (LOH) in lung cancers and that these studies have dealt with advanced lung cancer,[18] our findings of many losses in BAC and AdCa are understandable. The prevalence of the loss of chromosome 12 was significantly greater ($P < 0.01$) in well-differentiated AdCa < 1 cm than in BAC < 1 cm.

We encountered an interesting case of BAC surrounded by high-grade AAH (Fig. 1c, Table 4). The percentage of tumor cells having gain of chromosomes 4, 7, 9, 15, and 16 is higher in the central portion (BAC) than in the marginal region (AAH). We think this finding represents a stepwise progression of the CNA in the transition from adenomatous hyperplasia to BAC.

CNA features through tumor progression

We present the alteration of various chromosomes according to stage in Tables 5,6. The gain of chromosomes 7, 10, 12, 15 and 18 and the loss of chromosome 1, 2, 8, 9,10 and 16 seemed to be correlated with the progression of the stages.

As to the percentage of the tumor cells having five or more particular chromosomes, the prevalence was 0%, 0.14%, 0.20%, 0.80%, 0.68%, and 0.97% in normal lung; low-grade AHH; high-grade AHH; BAC; AdCa < 1 cm; and AdCa > 1 cm, respectively (details and a table not shown).

Table 4 Gain in a patient with BAC in high-grade AAH

Probe	Portion	Proportion (%)	P†
CEP1	Margin (AAH)	8	NS
	Center (BAC)	7	
CEP3	Margin (AAH)	10	NS
	Center (BAC)	9	
CEP4	Margin (AAH)	13	<0.01
	Center (BAC)	48	
CEP7	Margin (AAH)	10	<0.01
	Center (BAC)	53	
CEP9	Margin (AAH)	12	<0.01
	Center (BAC)	51	
CEP15	Margin (AAH)	1	<0.01
	Center (BAC)	11	
CEP16	Margin (AAH)	3	<0.01
	Center (BAC)	25	
CEP18	Margin (AAH)	7	NS
	Center (BAC)	20	
CEPX	Margin (AAH)	15	NS
	Center (BAC)	28	

AAH, atypical adenomatous hyperplasia; BAC, bronchioloalveolar carcinoma.

NS, not significant.

†Fisher's exact test.

Table 5 Gain according to stage

	Stage 1 (%)	a	Stage 2 + 3 (%)
CEP 1	30	>	16
CEP 2	26	>	10
CEP 3	24		20
CEP 4	29		33
CEP 6	22	>	14
CEP 7	17	<	40
CEP 8	21		23
CEP 9	21	>	8
CEP 10	14	<	24
CEP 11	18		15
CEP 12	15	<	29
CEP 15	12	<	14
CEP 16	30	>	12
CEP 17	28		27
CEP 18	12	<	19
CEP 20	22		32
CEP X	29		26
CEP Y	27	>	10
Average	23	>	21

[a]Fisher's exact test: $P < 0.01$.

>, greater in stage 1; <, greater in stage 2 + 3.

Mean ± SD (%) of gain, for stage 1 and stage 2 + 3: 22.078 ± 6.346; 20.611 ± 9.127, respectively.

Table 6 Loss according to stage

Probe	Stage 1 (%)	a	Stage 2 + 3 (%)
CEP 1	18	<	29
CEP 2	15	<	22
CEP 3	19		19
CEP 4	16		19
CEP 6	17		19
CEP 7	22	>	15
CEP 8	21	<	31
CEP 9	18	<	50
CEP 10	18	<	29
CEP 11	18		21
CEP 12	21		18
CEP 15	26		20
CEP 16	19	<	30
CEP 17	17		13
CEP 18	20		20
CEP 20	21		17
CEP X	13		14
CEP Y	11		12
Average	18	<	22

[a]Fisher's exact test: $P < 0.01$.

>, greater in stage 1; <, greater in stage 2 + 3.

Mean ± SD (%) of loss, for stage 1 and stage 2 + 3: 18.228 ± 3.358; 21.856 ± 9.057, respectively.

Table 7 Gain and clinicopathological characteristics of AdCa

	Gain (%)	P†
Male ($n = 10$)	24	<0.01
Female ($n = 18$)	21	
Smoker ($n = 7$)	18	<0.01
Non-smoker ($n = 21$)	23	
Well diff. AdCa > 1 cm ($n = 7$)	14	<0.01
Mod. diff. AdCa > 1 cm ($n = 7$)	25	
Poorly diff. AdCa > 1 cm ($n = 3$)	31	<0.01

AdCa, adenocarcinoma; diff., differentiated; mod., moderately.

Mean ± SD (%) of gain in male vs female; smoker vs non-smoker: 22.71 ± 9.99 vs 20.03 ± 11.47; 16.57 ± 7.29 vs 22.37 ± 11.52, respectively.

Mean ± SD (%) of gain for well diff., mod. diff., and poorly diff. : 13.57 ± 4.55; 23.06 ± 10.05; and 27.54 ± 12.26, respectively.

†Fisher's exact test.

CNA and individual parameters

Patient gender, smoking habit, tumor size and histological grade of AdCa were also analyzed with regard to CNA profile. The average of the gain in each category is shown in Table 7. Male patients had a higher incidence of CNA than female patients, as did non-smokers than smokers. CNA was exacerbated according to histological differentiation, and poorly differentiated AdCa had the highest degree of CNA. This difference existed even in the subanalysis of the AdCa < 1 cm (data not shown).

DISCUSSION

CNA is a well-known characteristic of lung cancer. Conventional karyotyping studies do not always reflect changes *in vivo* because *in vitro* expansion of particular clones and artificial chromosomal changes during the procedure may influence the results. The analysis of chromosomal abnormalities with FISH, such as in the present study, may reveal naturally occurring alterations and prevent miscalculation incorporating inflammatory and normal cell stromal contamination. Our technique facilitated the use of stored pathology

archives, especially those containing small lesions. A few chromosome-wide investigations in NSCLC with FISH have been reported.[11] As to AAH, there is only one report that examined four chromosomes with FISH.[12] In contrast, with regard to several other organs, there are reports stating that CNA already existed in premaligant lesions.[19–21] AAH in the lung has been considered to be a premalignant lesion of lung AdCa, especially of BAC, a particular pathological entity among AdCa.[17,22] In the present report we found that CNA do exist in AAH to a considerable degree. Alternately, the presence of CNA in AAH indicates its premalignant nature. This conclusion is also consistent with previous work using cytofluorometry.[23,24]

Substantial gain in chromosomes, not particularly specified, has been noted in most AAH. Zojer *et al.* reported a chromosome 7 abnormality among the four chromosomes they tested in a few AAH.[12] They noted that 5–21% of AHH cells had aneuploidy for chromosome 7 based on the data in four cases. In the present cases, 4–19% of AAH tumor cells had a gain of chtomosome 7. In the early phase of lung tumorigenesis, the gain of chromosomes was more conspicuous than loss, though we admit that the interpretation of the loss in this method is more difficult. Thus, the CNA in the present paper mostly refer to chromosome gain. And with regard to gain of chromosomes, the more susceptible chromosomes in the early phase of lung tumorigenesis were chromosomes 1, 2, 4, 6, 8, 16 and Y. Because there are no reports on CNA in lung tumors <1 cm, we cannot compare our data exactly with the previous reports. Previous papers have mainly dealt with advanced cases and used CGH. In contrast, the gain of chromosomes 1 and 8 has been documented in early phase gastric cancer,[25] therefore it is possible that these features are generally related to glandular epithelial proliferation in the early stage. In particular, the gain of chromosome 1 or 1q has been recognized by several methods including CGH in cancers of the lung,[26,27] breast, prostate, colon, endometrium and urinary bladder.

In the later stage of the present lung cancer series, the gains of chromosomes 7, 10, 12, 15 and 18 accumulated in tumor progression. As mentioned earlier, the gain of chromosome 7 in lung cancer has long been documented. In terms of this chromosome, our report here is also consistent with the previous karyotypic studies.[28–30] The gains of chromosomes 10, 15 and 18 have also been documented in advanced gastric cancer.[25] If CNA are indeed a cause of tumorigenesis and increase the incidence of cancer, this result supports the idea that male subjects have a higher incidence in all cancer types except for thyroid, breast and other female organs.

A gradual increase of CNA was observed from normal epithelial cells to low-grade AAH, high-grade AAH and, finally, to BAC, in this order. But once a cell acquired a recognizable malignant transformation, there seemed to be no further stepwise aggravation from BAC to AdCa ≤ 1 cm with regard to chromosomal gain. In addition, there was no further aggravation of the gain throughout stage progression after the tumor passed the size of 1 cm. This result is consistent with the results from flow cytometric analysis that found that the DNA content in NSCLC had been unrelated to tumor progression.[31] The chromosome aberration had nearly stabilized in advanced breast cancer also.[32,33] This could be compared to the situation in squamous cell carcinogenesis of the lung, where a great difference exists between precancerous lesions and *in situ* carcinoma.[34] The most critical temporal point in lung carcinogenesis seems to be the transition from AAH to small BAC in adenocarcinoma and precancerous bronchial mucosa, to *in situ* carcinoma in squamous cell carcinoma.

However, an alternate interpretation from Table 2 may provide a trend of increase in chromosomes (in which the prevalence of CNA is very high, e.g. >28%) from AAH to AdCa. Further analysis as to more specific changes covering the genome-wide loci will refine the whole picture of this sequence, including chromosomal evolution.[35] MW-assisted FISH using various bacterial artificial chromosome probes would also help this refinement.[36]

CNA, both gains and losses, seem to occur both differently and concurrently in the temporal spectrum of lung carcinogenesis. In particular, after the tumor exhibits overt carcinoma (BAC and later), both gains and losses can occur, and we could not detect any unidirectional tendency. And when we calculate the average frequency of the gain in BAC < 1 cm, AdCa < 1 cm and AdCa > 1 cm, we found that they were all the same, approximately 20%. If cancer was to have its origin in one cell that acquired a CNA, the point at which 20% of the cells become aneuploidal might be a 'tipping point'[37] of carcinogenesis, where cancer cells establish themselves.

In contrast, extraordinary gains (five or more) seem to increase according to this process, from AHH to AdCa > 1 cm, and the significance of this observation remains to be investigated.

In this argument we must note that the FISH method is more useful for estimating gain than loss. The average of the loss in the control reached 21% whereas that of gain was 1%. Obviously combinations of other methods such as LOH, CGH and oligonucleotide microarray will further clarify the details of molecular initiation and progression of lung cancer.

The consequential acquisition of the CNA, especially a gain, would give precancerous cells the excellent opportunity to alter their characteristics. One is to gain a more selective growth advantage by losing a chromosome that harbors tumor suppressor genes following LOH,[35] and the other is to obtain additional chromosomes (polysomy) that harbor growth-promoting genes.[38] The fact that aneusomy was observed through tumor initiation supports the idea that

cancer initiation and progression depend on altered dosages of thousands of genes resulting from aneuploidy, rather than particular cancer-related genes.[39]

Our report shows that AAH, a premalignant lesion of AdCa, already has a CNA encompassing considerable numbers of different chromosomes. One cancer cell is derived from a group of precancerous cells that already acquired CNA and consequently continues to generate a new phenotype. Interestingly, in one case in which there was a central portion with a higher dysplastic grade surrounded by a less dysplastic field, a stepwise increase in the CNA was observed, as depicted in the schematic picture of Fig. 2. This phenomenon reminds us of the analogous concept of 'mutation load'[40] in the cancer field. We now propose 'chromosomal aberration load' from low-grade AAH (Fig. 3a) to high-grade AAH (Fig. 3b) and finally to BAC (Fig. 3c).

Many investigators favor the alternative mutation-driven scenario including K-ras (chromosome 12) and EGFR (chromosome 7) mutations.[41] We must await further research before we can know whether our view complements theirs.

ACKNOWLEDGMENTS

The authors would like to thank Ms K. Nagura of the Hamamatsu University School of Medicine, Japan, for technical assistance concerning the FISH analysis. This work was supported in part by a Grant-in-Aid from the Ministry of Health, Labour and Welfare (15-5 and 15-22), from the Ministry of Education, Culture, Sports, Science (17015017, 15390125) and Technology of Japan for Scientific Research on Priority Area, from the 21st century COE program 'Medical Photonics', from the Smoking Research Foundation, and from the Foundation for Promotion of Cancer Research. We thank Professor Noguchi at Tsukuba University for critical comments on the manuscript.

REFERENCES

1 Fearon ER, Vogelstein B. A genetic model for colorectal tumorigenesis. *Cell* 1990; **61**: 759–67.
2 Charames GS, Bapat B. Genomic instability and cancer. *Curr Mol Med* 2003; **3**: 589–96.
3 Komarova NL, Lengauer C, Vogelstein B, Nowak MA. Dynamics of genetic instability in sporadic and familial colorectal cancer. *Cancer Biol Ther* 2002; **1**: 685–92.
4 Lengauer C, Kinzler KW, Vogelstein B. Genetic instability in colorectal cancers. *Nature* 1997; **386**: 623–7.
5 Nowak MA, Komarova NL, Sengupta A *et al.* The role of chromosomal instability in tumor initiation. *Proc Natl Acad Sci USA* 2002; **99**: 16 226–31.
6 Bialy H. Aneuploidy and cancer: The vintage wine revisited. *Nat Biotechnol* 2001; **19**: 22–3.
7 Duesberg P, Li R. Multistep carcinogenesis: A chain reaction of aneuploidizations. *Cell Cycle* 2003; **2**: 202–10.
8 Pihan G, Doxsey SJ. Mutations and aneuploidy: Co-conspirators in cancer? *Cancer Cell* 2003; **4**: 89–94.
9 Haigis KM, Caya JG, Reichelderfer M, Dove WF. Intestinal adenomas can develop with a stable karyotype and stable microsatellites. *Proc Natl Acad Sci USA* 2002; **99**: 8927–31.
10 Marx J. Debate surges over the origins of genomic defects in cancer. *Science* 2002; **297**: 544–6.
11 Taguchi T, Zhou JY, Feder M, Litwin S, Klein-Szanto AJ, Testa JR. Detection of aneuploidy in interphase nuclei from non-small cell lung carcinomas by fluorescence in situ hybridization using chromosome-specific repetitive DNA probes. *Cancer Genet Cytogenet* 1996; **89**: 120–25.
12 Zojer N, Dekan G, Ackermann J *et al.* Aneuploidy of chromosome 7 can be detected in invasive lung cancer and associated premalignant lesions of the lung by fluorescence in situ hybridisation. *Lung Cancer* 2000; **28**: 225–35.
13 Kitayama Y, Igarashi H, Sugimura H. Initial intermittent microwave irradiation for fluorescence in situ hybridization analysis in paraffin-embedded tissue sections of gastrointestinal neoplasia. *Lab Invest* 2000; **80**: 779–81.
14 Kitayama Y, Igarashi H, Sugimura H. Different vulnerability among chromosomes to numerical instability in gastric carcinogenesis: Stage-dependent analysis by FISH with the use of microwave irradiation. *Clin Cancer Res* 2000; **6**: 3139–46.
15 Sobin LH, Fleming ID. TNM classification of malignant tumors, 5th edn. Union Internationale Contre le Cancer and the American Joint Committee on Cancer. *Cancer* 1997; **80**: 1803–4.
16 Travis W, Colby T, Corrin B, Shimosato Y, Brambilla E, Sobin L. *Histological Typing of Lung and Pleural Tumors*. Berlin: Springer, 1999.
17 Koga T, Hashimoto S, Sugio K *et al.* Lung adenocarcinoma with bronchioloalveolar carcinoma component is frequently associated with foci of high-grade atypical adenomatous hyperplasia. *Am J Clin Pathol* 2002; **117**: 464–70.
18 Tseng RC, Chang JW, Hsien FJ *et al.* Genomewide loss of heterozygosity and its clinical associations in non small cell lung cancer. *Int J Cancer* 2005; **117**: 241–7.
19 Ai H, Barrera JE, Meyers AD, Shroyer KR, Varella-Garcia M. Chromosomal aneuploidy precedes morphological changes and supports multifocality in head and neck lesions. *Laryngoscope* 2001; **111**: 1853–8.
20 Duesberg P, Li R, Rasnick D *et al.* Aneuploidy precedes and segregates with chemical carcinogenesis. *Cancer Genet Cytogenet* 2000; **119**: 83–93.
21 Rabinovitch PS, Dziadon S, Brentnall TA *et al.* Pancolonic chromosomal instability precedes dysplasia and cancer in ulcerative colitis. *Cancer Res* 1999; **59**: 5148–53.
22 Mori M, Rao SK, Popper HH, Cagle PT, Fraire AE. Atypical adenomatous hyperplasia of the lung: A probable forerunner in the development of adenocarcinoma of the lung. *Mod Pathol* 2001; **14**: 72–84.
23 Nakayama H, Noguchi M, Tsuchiya R, Kodama T, Shimosato Y. Clonal growth of atypical adenomatous hyperplasia of the lung: Cytofluorometric analysis of nuclear DNA content. *Mod Pathol* 1990; **3**: 314–20.
24 Yokozaki M, Kodama T, Yokose T, Matsumoto T, Mukai K. Differentiation of atypical adenomatous hyperplasia and adenocarcinoma of the lung by use of DNA ploidy and morphometric analysis. *Mod Pathol* 1996; **9**: 1156–64.
25 Kitayama Y, Igarashi H, Sugimura H. Nonrandom chromosomal numerical abnormality predicting prognosis of gastric cancer. A retrospective study of 51 cases using pathology archives. *Lab Invest* 2003; **83**: 1–10.
26 Goeze A, Schluns K, Wolf G, Thasler Z, Petersen S, Petersen I. Chromosomal imbalances of primary and metastatic lung adenocarcinomas. *J Pathol* 2002; **196**: 8–16.

27 Petersen I, Hidalgo A, Petersen S *et al.* Chromosomal imbalances in brain metastases of solid tumors. *Brain Pathol* 2000; **10**: 395–401.
28 Matturri L, Lavezzi AM. Recurrent chromosome alterations in non-small cell lung cancer. *Eur J Histochem* 1994; **38**: 53–8.
29 Testa JR, Siegfried JM, Liu Z *et al.* Cytogenetic analysis of 63 non-small cell lung carcinomas: Recurrent chromosome alterations amid frequent and widespread genomic upheaval. *Genes Chromosomes Cancer* 1994; **11**: 178–94.
30 Lukeis R, Ball D, Irving L, Garson OM, Hasthorpe S. Chromosome abnormalities in non-small cell lung cancer pleural effusions: Cytogenetic indicators of disease subgroups. *Genes Chromosomes Cancer* 1993; **8**: 262–9.
31 Sahin AA, Ro JY, el-Naggar AK *et al.* Flow cytometric analysis of the DNA content of non-small cell lung cancer. Ploidy as a significant prognostic indicator in squamous cell carcinoma of the lung. *Cancer* 1990; **65**: 530–37.
32 Kuukasjarvi T, Tanner M, Pennanen S, Karhu R, Kallioniemi OP, Isola J. Genetic changes in intraductal breast cancer detected by comparative genomic hybridization. *Am J Pathol* 1997; **150**: 1465–71.
33 Kuukasjarvi T, Karhu R, Tanner M *et al.* Genetic heterogeneity and clonal evolution underlying development of asynchronous metastasis in human breast cancer. *Cancer Res* 1997; **57**: 1597–604.
34 Wistuba II, Lam S, Behrens C *et al.* Molecular damage in the bronchial epithelium of current and former smokers. *J Natl Cancer Inst* 1997; **89**: 1366–73.
35 Varella-Garcia M, Gemmill RM, Rabenhorst SH *et al.* Chromosomal duplication accompanies allelic loss in non-small cell lung carcinoma. *Cancer Res* 1998; **58**: 4701–7.
36 Igarashi H, Yamashita K, Suzuki M *et al.* Simultaneous imaging of membrane antigen and the corresponding chromosomal locus in pathology archives. *Pathol Int* 2005; **55**: 753–6.
37 Gladwell M. *The Tipping Point: How Litlte Things Can Make a Big Difference.* New Port Beach: Back Bay Books, 2002.
38 Lengauer C, Kinzler KW, Vogelstein B. Genetic instabilities in human cancers. *Nature* 1998; **396**: 643–9.
39 Stock RP, Bialy H. The sigmoidal curve of cancer. *Nat Biotechnol* 2003; **21**: 13–14.
40 Hussain SP, Harris CC. p53 mutation spectrum and load: The generation of hypotheses linking the exposure of endogenous or exogenous carcinogens to human cancer. *Mutat Res* 1999; **428**: 23–32.
41 Yoshida Y, Shibata T, Kokubu A *et al.* Mutations of the epidermal growth factor receptor gene in atypical adenomatous hyperplasia and bronchioloalveolar carcinoma of the lung. *Lung Cancer* 2005; **50**: 1–8.